

Article

Influence of Multi-Period Tectonic Movement and Faults on Shale Gas Enrichment in Luzhou Area of Sichuan Basin, China

Xuwen Shi ¹, Wei Wu ¹, Yuguang Shi ^{2,3,*} , Zhenxue Jiang ^{2,3}, Lianbo Zeng ², Shijie Ma ², Xindi Shao ^{2,3}, Xianglu Tang ^{2,3} and Majia Zheng ¹

¹ Shale Gas Research Institute of Petrochina Southwest Oil & Gas Field Company, Chengdu 610051, China

² State Key Laboratory of Petroleum Resources and Prospecting, China University of Petroleum, Beijing 102249, China

³ Unconventional Oil and Gas Science and Technology Research Institute, China University of Petroleum, Beijing 102249, China

* Correspondence: 15639294976@163.com

Abstract: The Luzhou area in the southern Sichuan Basin has experienced multiple tectonic movements, forming a complex fault system; the activity has an important impact on the enrichment of shale gas in this area. In order to reveal the influence of the fracture system on the differential enrichment of shale gas, this paper takes the southern Sichuan Basin as the research object. The structural evolution process and fracture development characteristics of the different tectonic units in Luzhou area of southern Sichuan were characterized by conducting a seismic profile analysis, structural recovery using a back-stripping method, and core hand specimen description. We clarified the control effect of the structural deformation and fracture on the differential enrichment of shale gas, and we established a differential enrichment model of shale gas in the Luzhou area. The results show that: (1) The Luzhou area has undergone the transformation of a multi-stage tectonic movement. There are many sets of detachment structures in the longitudinal direction, and the plane structural form is a thin-skin fold-thrust belt composed of wide and narrow anticlines in the north–south direction. (2) The faults in the study area are affected by the Himalayan tectonic movement. The high-angle reverse faults are developed, and the number of large faults is small. The second and third faults are mainly developed. The second faults are only developed at the high position of the structure, which has a significantly destructive effect on shale gas reservoirs, while the third and fourth faults have no significant destructive effect on shale gas reservoirs. (3) In the study area, the types of cracks are categorized into transformational shear cracks, bed-parallel shear cracks, intraformational open cracks, lamellation cracks, shrinkage cracks, and abnormal high-pressure cracks. The thickness of the shale rock mechanical layer, brittle mineral content, and organic matter content jointly control the crack development degree in the shale of the Wufeng–Longmaxi Formation. (4) The uplift erosion, structural deformation, and fracture development caused by the structural evolution have affected the preservation of shale gas, resulting in the differential enrichment of shale gas reservoirs in the region. Based on the enrichment factors of shale gas, we established a differential enrichment model of shale gas in typical structural units and optimized the favorable enrichment areas, which are important contributions for guiding shale gas exploration and development in the Sichuan Basin.

Keywords: differential enrichment; shale gas; fracture system; tectonic movement; Sichuan Basin



Citation: Shi, X.; Wu, W.; Shi, Y.; Jiang, Z.; Zeng, L.; Ma, S.; Shao, X.; Tang, X.; Zheng, M. Influence of Multi-Period Tectonic Movement and Faults on Shale Gas Enrichment in Luzhou Area of Sichuan Basin, China. *Energies* **2022**, *15*, 6846. <https://doi.org/10.3390/en15186846>

Academic Editor: Manoj Khandelwal

Received: 30 July 2022

Accepted: 14 September 2022

Published: 19 September 2022

Publisher's Note: MDPI stays neutral with regard to jurisdictional claims in published maps and institutional affiliations.



Copyright: © 2022 by the authors. Licensee MDPI, Basel, Switzerland. This article is an open access article distributed under the terms and conditions of the Creative Commons Attribution (CC BY) license (<https://creativecommons.org/licenses/by/4.0/>).

1. Introduction

Since the shale gas revolution in North America that made important breakthroughs in the exploration and development of the resource, shale gas has attracted wide attention worldwide. As an important low-carbon clean energy, shale gas has become one of the important replacement targets for the exploration of oil and gas. China's shale gas is mainly produced in the southern Sichuan Basin and the surrounding Wufeng–Longmaxi

Formation [1–5]. As of December 2021, the cumulative proven geological reserves of shale gas in the Wufeng–Longmaxi Formation were estimated to be about $2.73 \times 10^{12} \text{ m}^3$ and the annual production of shale gas exceeded $230 \times 10^8 \text{ m}^3$. China's shale gas exploration has made significant progress [6–9]. The shale gas in the Sichuan Basin and its surrounding Wufeng–Longmaxi Formation has formed an industrial development system, and three shale gas demonstration zones, Changning–Weiyuan, Zhaotong, and Fuling, have been built. Blocks such as the Luzhou and Dazu areas have gradually become the replacement blocks for shale gas production [10–12].

Previous studies have made important progress on defining the static characteristics of preservation conditions for shale gas in the Longmaxi Formation in southern Sichuan; however, the research on the dynamic evolution of preservation conditions and the coupling control mechanism of shale gas enrichment under different scale preservation conditions is still relatively weak [13–15]. The southern Sichuan area has experienced multi-stage and multi-cycle tectonic movements since the Paleozoic Era [16]. The tectonic evolution process is complex, and the associated fracture patterns are diverse. Different structural combinations, structural styles, and parts have different enrichment and control effects on shale gas, resulting in significant differences in the gas content and production of shale gas reservoirs under different tectonic backgrounds [17,18]. There are many types of rich shale gas structures in the southern Sichuan Basin. The enrichment factors and patterns of shale gas in different structures are made different by the influence of various genetic mechanisms [19,20]. Therefore, it is still an urgent problem to clarify how to develop the structural deformation and evolution characteristics of the Luzhou area in southern Sichuan, how to determine the main controlling factors of fracture development in the Luzhou area, and how to jointly affect the enrichment and accumulation of shale gas by macroscopic tectonic movement and microscopic fracture development.

This study took the Luzhou area in southern Sichuan as the research object and conducted a seismic profile analysis, tectonic restoration using a back-stripping method, and core hand specimen description to finely characterize the tectonic evolution process and fault development characteristics of the typical tectonic units in the Luzhou area. We clarified the control effect of the tectonic movement and fracture development on the differential enrichment of shale gas. Compared with the predecessors, the influence of tectonic evolution on the enrichment of shale gas in the later preservation is emphasized. Finally, we establish a model of differential enrichment of shale gas in Luzhou area of southern Sichuan, which provides a theoretical guidance and technical support for the exploration and development of deep shale gas in Luzhou area.

2. Geological Settings

The Sichuan Basin is a typical superimposed basin that is characterized by a multi-stage tectonic movement superposition. The Sichuan Basin starts from the Longmen Shan fold belt in the west, the Qiyue Shan fold belt in the east, the Micang Shan uplift and the Daba Shan fold belt in the north, and the Emei–Liangshan fold belt in the south. The Luzhou area is located in the southern Sichuan Basin and is tectonically located in the south Sichuan low-steep tectonic belt between the middle Sichuan paleouplift and the southeast Sichuan fold belt [21] (Figure 1). The multi-stage tectonic movement experienced by the low-steep structural belt in the southern Sichuan region has led to the development of a series of typical NS-trending high-steep anticlines and wide-gentle synclines, with typical complex fold characteristics. During the Yangtze cycle, the stable crystalline basement was formed in the Luzhou area under the strong influence of Jining movement. The Caledonian movement occurred, and the Sichuan Basin showed a pattern of large uplift and depression as a whole. The northern part of southern Sichuan began to uplift, and the southern part produced the central Guizhou uplift and the Sichuan–Guizhou depression. The Hercynian movement caused the erosion of the early sedimentary layer, and some Silurian, Devonian, and Carboniferous layers were missing from bottom to top. In the Late Indosinian, the area entered the foreland basin evolution stage; in the early Yanshanian, the

strong tectonic movement formed the Huaying Shan fault zone and local uplift, resulting in a small-scale uplift of the low-steep structural belt in southern Sichuan. The Himalayan tectonic movement led to a significant uplift in southern Sichuan, resulting in a strong erosion of strata and a lack of Paleogene and Neogene strata [22,23].

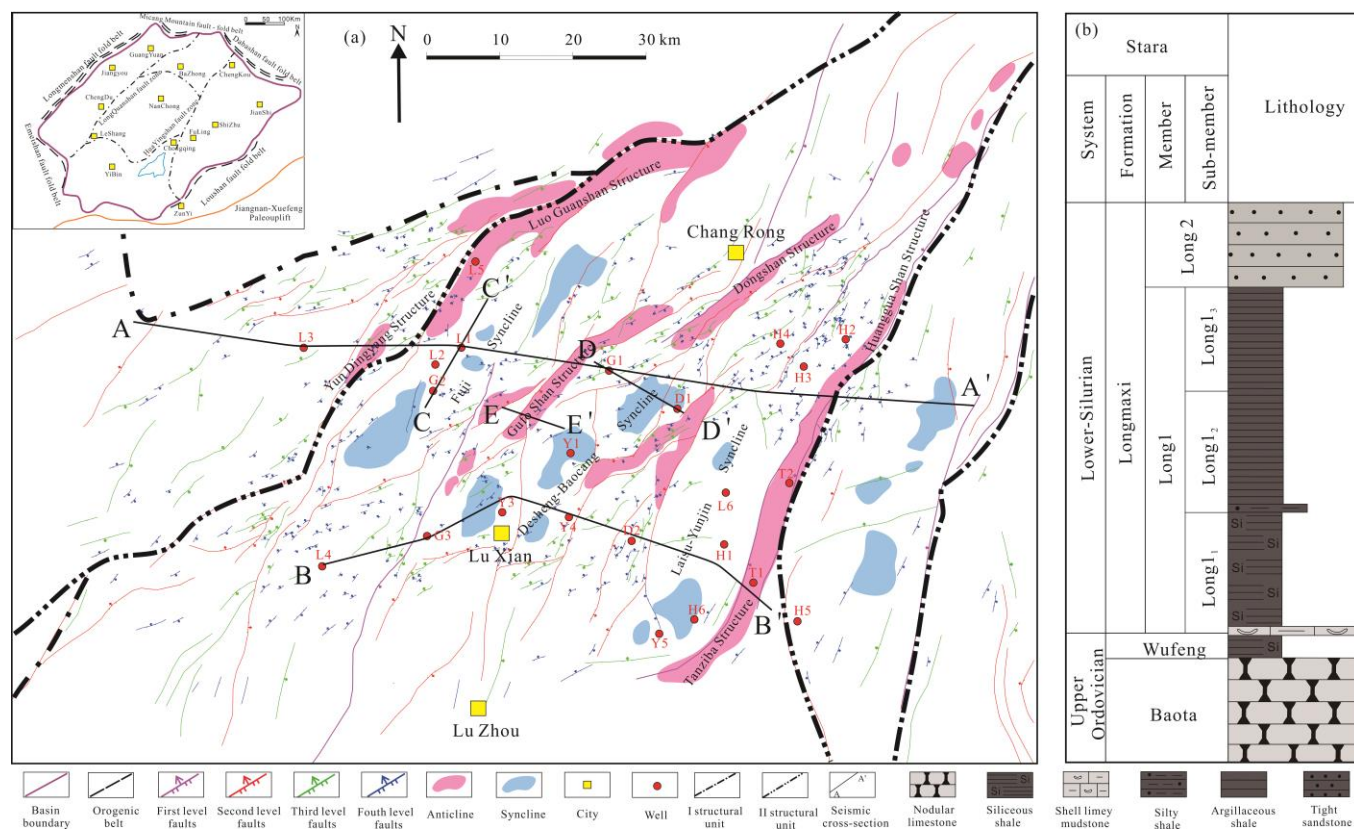


Figure 1. The regional tectonic positioning. (a) The regional geology of the Luzhou area; (b) a regional stratigraphic comprehensive histogram.

The Wufeng–Longmaxi Formation shale that formed from the late Ordovician to the early Silurian is the main layer for shale gas exploration and development in the Luzhou area. The sedimentary thickness is between 500 m and 650 m. The bottom of the Wufeng Formation is integrated with the limestone of the underlying Linxiang Formation, and the top is integrated with the upper Longmaxi Formation. The top of the Longmaxi Formation is integrated with the carbonate rocks of the lower Silurian Shiniulan Formation. The bottom of the Longmaxi Formation is rich in biogenic siliceous minerals, with a mass fraction of 60–70%. The TOC mass fraction of shale is 2.8–6.0%, with an average of 3.9%. The porosity is 4.0–6.5%, with an average of 5.1%. The gas saturation is 50–70%, with an average of 65%. The total gas content recovered based on field tests is 5.0–7.5 m³/t, with an average of 6.3 m³/t, which is the highest in southern Sichuan [24–26].

3. Sample Selection and Experimental Method

The experimental samples in this paper were collected from black shale samples of the Wufeng–Longmaxi Formation from 12 wells in the Luzhou area, southern Sichuan Basin (Table 1). The cracks on the core specimens were classified and described to uncover the cause, density, and production of the cracks. The crack stages and time were divided by combining the intersecting relationship of cracks on the core with the burial history experiment. The organic carbon content and gas content of all samples were tested. The well location is shown in Figure 1.

Table 1. Experimental Sample Number, Well Name, and Formation.

Number	Well	Formation	Depth/m
1	L1	Longmaxi	3799.50
2	L2	Longmaxi	3724.18
3	L2	Wufeng	3755.60
4	L3	Wufeng	4036.53
5	L4	Wufeng	4053.18
6	L5	Longmaxi	3395.87
7	L5	Wufeng	3461.67
8	L6	Longmaxi	4280.80
9	Y1	Longmaxi	4150.10
10	Y2	Longmaxi	4146.83
11	Z1	Wufeng	4108.85
12	G1	Longmaxi	3679.00
13	Y3	Longmaxi	3847.70
14	H1	Longmaxi	4289.60

3.1. Gas Content and X-ray Diffraction Analysis

Shale gas content recovery was conducted using USBM method, where the test sample is the full diameter core, the core height is about 30 cm, and the test instrument is a shale field gas content test device [27].

The whole rock minerals and clay minerals were analyzed and detected by a D8AA25 X-ray diffractometer (Bruker AXS, Karlsruhe, Germany). The whole rock mineral samples were crushed and ground to be below 40 μm grain size, where they were then pressed into tablets by a back-pressure method. The diffraction spectra of 3–45° were obtained on a computer. The content data of various minerals were calculated according to the corresponding formula in the standard and the mineral K value. For the relative content analysis of clay minerals, the samples were crushed to a 1 mm particle size, were soaked and dispersed, and less than 5 μm (sandstone) and 2 μm (mudstone) particles were extracted to make natural slices. The diffraction spectrum of 2.5–15° (2 θ angle) was obtained on a computer. The relative content data of clay minerals were calculated according to the formula in the standard.

3.2. Test of Porosity

An UltraPore-200 Helium Porosity Meter (American Core Temco Company, Clackamas, OR, USA) was used to measure the porosity of samples. In principle according to Boyle's law $P_1V_1 = P_2V_2$, helium gas was used as the test gas, which has poor adsorption performance and small molecules. The particle volume and pore volume were measured by the double-chamber and single-chamber methods, respectively. Then the porosity was calculated, that is, the known P_1 and V_1 , measured P_2 , and calculated V_2 .

3.3. Organic Carbon Content

The total organic carbon (TOC) measurement of shale samples was taken using a CS-344 carbon sulfur analyzer (American LECO Company, St. Joseph, MI, USA). Before the experiment, the surface of the sample was washed using an ultrasonic vibration, and then the sample was crushed and ground to be below 80 meshes (198 μm). The sample was then treated using the chemical method. The 100 mg crushed whole rock sample was weighed and treated with 5% of HCl for 24 h. During the reaction, carbon dioxide was released, and the inorganic carbon component was removed. Then, the total organic carbon was converted into carbon dioxide through combustion in a high-temperature oxygen flow, and the organic carbon content was detected and tested by the infrared detector.

3.4. Simulation of Strata Burial History and Reconstruction Technique of Structural Balance Profile

A burial history simulation is an important basis for studying shale gas reservoirs. The purpose of burial history recovery is to analyze the development and evolution of ancient structures and to define the geological history period. Based on the single well stratigraphic sequence, thickness, lithology data, recovery of erosion, and other related parameters, we used PetroMod 2012.2 oil system simulation software, developed by the company IES (Germany), to restore the burial history. The technique of a balanced profile is based on the law of conservation of matter. For a profile, the shortening of the profile is made consistent with the thickening of the stratum to keep the area of the profile unchanged. The theorem of layer length conservation is simplified on the basis of area conservation; at present, this method is widely used in profile balancing. In this paper, 2Dmove software was used to compile the balanced profile. Firstly, a geological (depth) or seismic (time) section is detailed to establish the geological model of the area, and then the influence of fault distance is eliminated to invert the structural development history.

4. Results and Discussion

4.1. Structural Deformation and Evolution Characteristics

4.1.1. Superimposed Structural Deformation Characteristics

Structural traces in the NE–SW, NW–SE, E–W, and N–S directions have developed in the Luzhou area. The northeast area of Luzhou is dominated by NE–S-trending tectonic traces and changes into NW–SE when transitioning to the south-west; the N–S-trending tectonic traces evolve into E–W-trending tectonic traces when approaching the southernmost part of Luzhou. There is an obvious superposition deformation of three groups of structural traces in different directions in the Luzhou area. The NW–SE-trending structural traces are obviously controlled by the NE–SW-trending structural traces, and the arc distortion occurs at the fold hinge at the turning point of the structural traces. The NE–SW-trending structural traces are slightly cut by the NW–SE-trending structural traces, and no obvious fault occurs. Combined with the results of the superimposed structural deformation, it can be concluded that the formation time of the NE–SW-trending structural trace is the earliest, the formation time of E–W-trending structural trace is later, and the formation time of nearly N–S-trending structural trace is the most recent [28] (Figure 2).

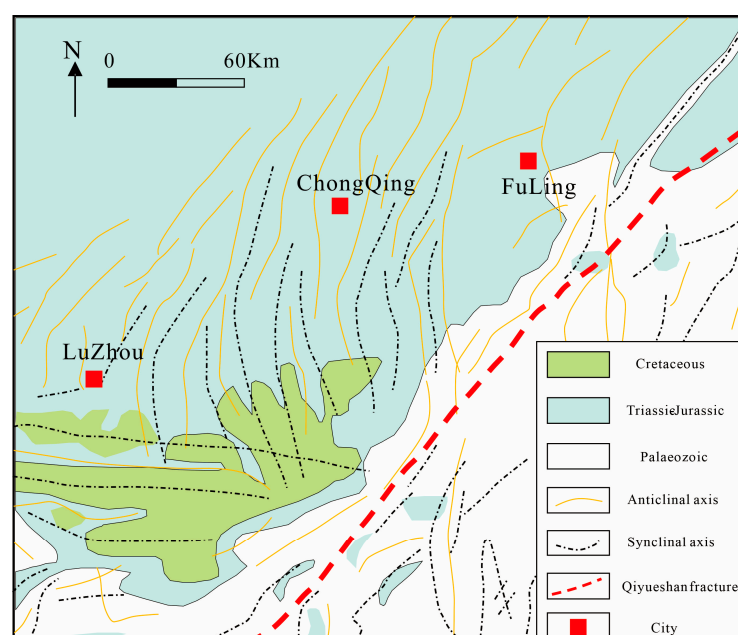


Figure 2. Outline of the structural plane in southeast Sichuan.

4.1.2. Plane Structural Style

Affected by the basement fault of Qiyue Shan in the east of Luzhou and controlled by the NW–SE-trending tectonic stress field, brush folds formed in the north of Luzhou and ended in the Qiyue Shan fault. At the end of the brush folds, a thin-skin fold-thrust belt formed under the control of the E–W-oriented tectonic stress field, with an NW–SE wide syncline and a narrow anticline. Driven by the north–south tectonic stress, the south of Luzhou has formed a nearly E–W-trending thin-skin fold-thrust belt. From south to north, it presents a plane structural pattern of ‘nearly E–W-trending thin skin fold-thrust belt, nearly N–S-trending parallel fold structure group and brush folds’ [29] (Figure 2).

4.1.3. Profile Structural Style

The Luzhou area is characterized by ejective composite folds. According to the tectonic detachment structure, the Luzhou area can be vertically divided into the upper deformation layer, middle deformation layer, and lower deformation layer, which is bounded by the Middle-Lower Cambrian gypsum salt rock, Longmaxi Formation shale, and Jialingjiang Formation gypsum salt rock. It can be concluded from the section that the tectonic reformation intensity of the medium deformed structural layer is the strongest, and there are four structural styles, including the imbricate thrust, hedge thrust, back thrust, and Y-shaped large fault. The structural transformation intensity of the upper deformed structural layer is the weakest, and there are two kinds of structural styles, hedging thrust and back thrust, that have locally developed. On the whole, the pattern of ‘vertical stress difference controlled by slip structure and combination of structural styles controlled by stress difference’ is presented (Figure 3).

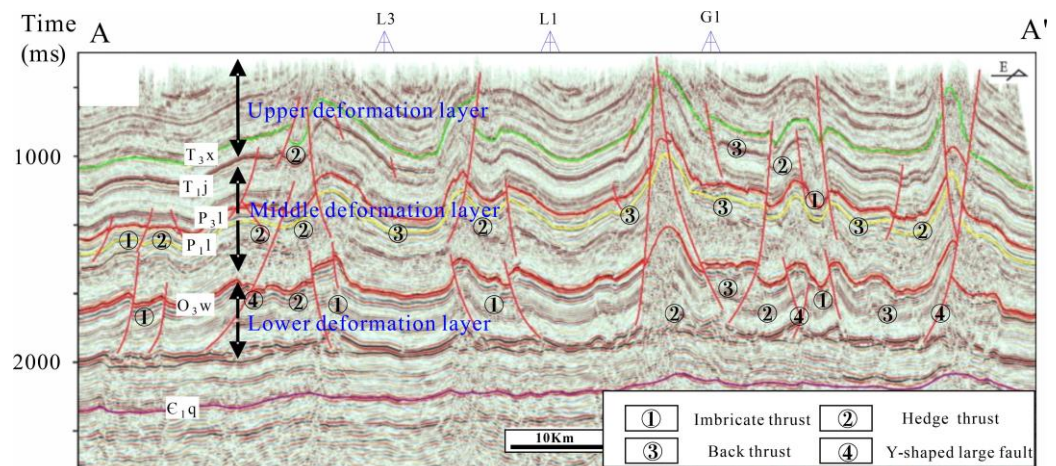


Figure 3. The interpretation section of the structural style in the Luzhou area (see Figure 1 AA’).

4.1.4. Tectonic Evolution Process

The evolution process of the geological and historical structure in the Luzhou area was determined by means of a series of techniques, including the leveling, back-stripping, and decompaction of the balanced profile. From the Caledonian to the early Indosinian, the Luzhou area was mainly in the background of the uplift erosion and extension, with less fault development and simple normal faults, forming part of the graben structure. In the middle and late Indosinian, the long-distance transmission effect from the compressive stress of the Jiangnan–Xuefeng orogenic belt to the northwest resulted in the structural inversion in the Luzhou area and the prototype formation of the Luzhou paleouplift. The main body was NE-trending and its range was expanding to the northwest and southeast sides. In the early Yanshanian, the NW–SE-trending compression from the Xuefeng Shan affected the East Sichuan fold belt, forming NE–SW-trending folds and faults in the central part. Under the strong influence of the late Yanshanian, the NW-trending compression continued, and at the same time, it was subjected to the nearly N–S-trending compression,

forming NE–SW-trending, E–W-trending, and nearly N–S-trending structures. Most anticlines had multiple faults to form fault cut-through folds and fault propagation folds, as well as hedging structures and anticlines. The large-scale uplift occurred in the strata. The nearly S–N fault experienced a multi-stage deformation, and the nearly E–W compression deformation in Himalayan period strongly reformed the fault. Then, the surface was further eroded and transformed to form the present topography [30,31] (Figure 4).

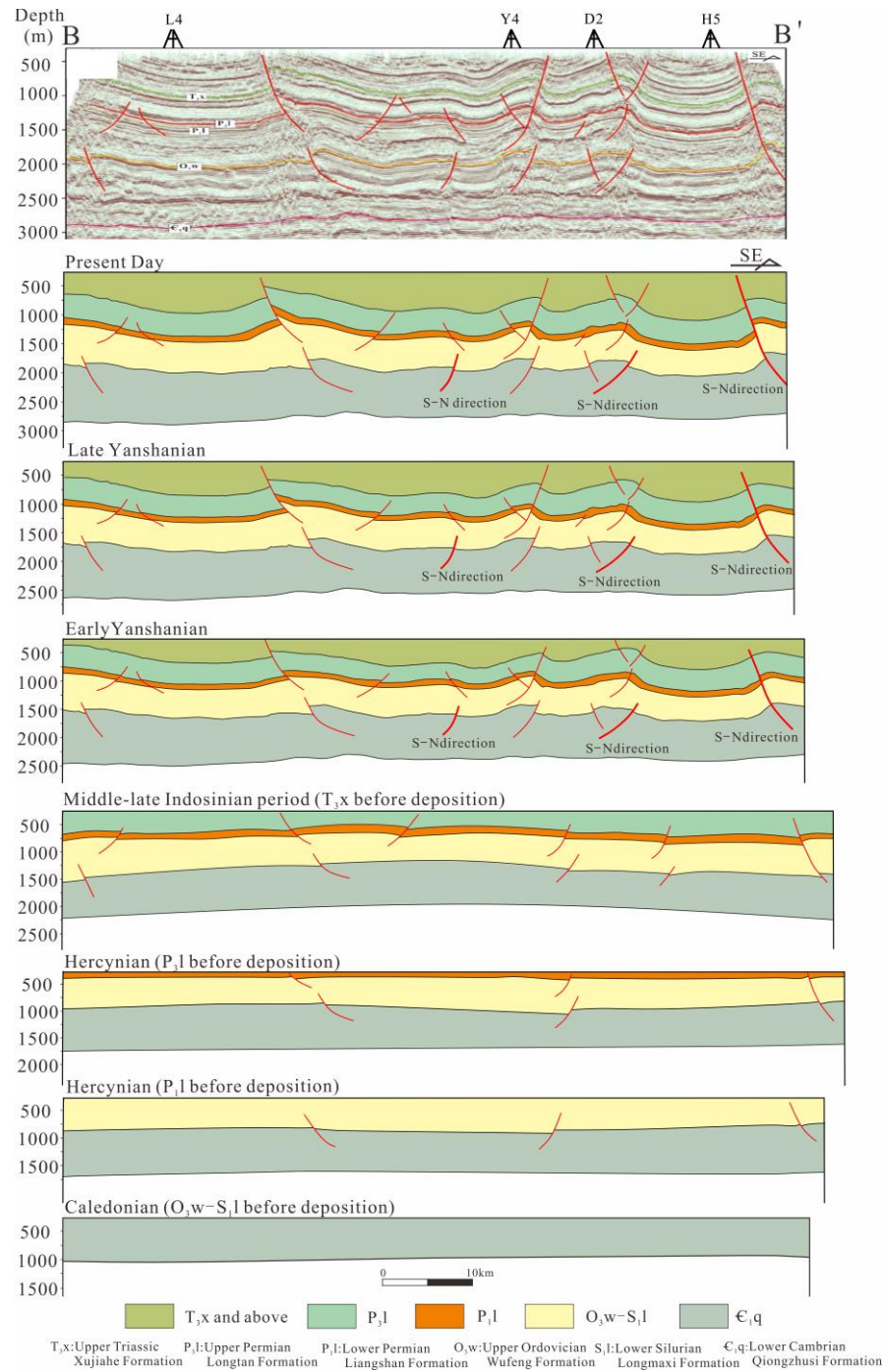


Figure 4. The tectonic evolution section of the Luzhou area (see Figure 1 BB’).

4.2. Fracture Development Characteristics and Main Controlling Factors

4.2.1. Development Characteristics of Faults

NE–SW-trending faults are mainly developed in the Luzhou area, with nearly E–W and nearly S–N-trending faults. The NE–SW faults experienced an extrusion deformation in the early Yanshanian, late Yanshanian, and Himalayan periods (Figure 5a). The nearly E–W-trending faults underwent a compression deformation in the late Yanshanian and Himalayan periods (Figure 5b). The nearly S–N fault experienced a compression deformation in the early Yanshanian, late Yanshanian, and Himalayan periods, among which the Himalayan tectonism resulted in the most intense transformation (Figure 5c).

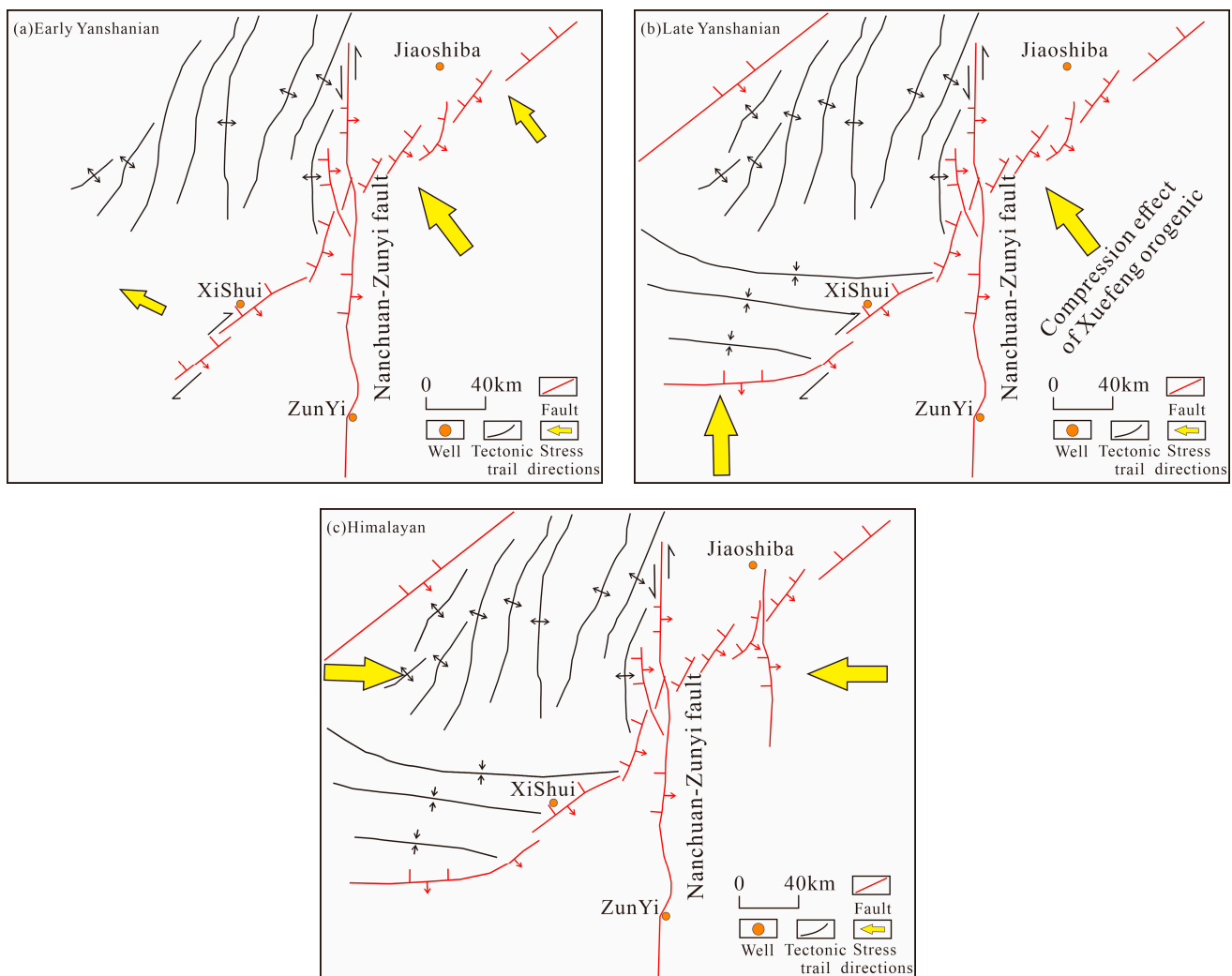


Figure 5. The distribution characteristics of faults in different periods. (a) Distribution of the early Yanshanian fault; (b) distribution of late Yanshanian fault; (c) distribution of late Himalayan fault.

The Luzhou area is characterized by a layered deformation. The high-angle reverse faults control the most deep and shallow anticlines, and partially cut through the plastic layers, forming large faults. The profile A–A' (Figure 6) (through wells L3, L1, H3) in the northern part of the Luzhou area shows that the northern part of the Luzhou area mainly develops ejective folds with a combination of wide-slow synclines and anticlines, showing a deep-shallow layered deformation, with two sets of plastic layers. The main fault is the high-angle reverse fault, and some large faults cut through the plastic layer. Section B–B' (Figure 6) (through well L4 and Y4) across the southern part of Luzhou shows that the southern part of Luzhou is also dominated by the development of ejective folds. The

tectonic deformation intensity is weaker than that of the northern part, as is the deformation of the deep and shallow layers. The main fault is the high-angle reverse fault, and there are fewer developments of large faults.

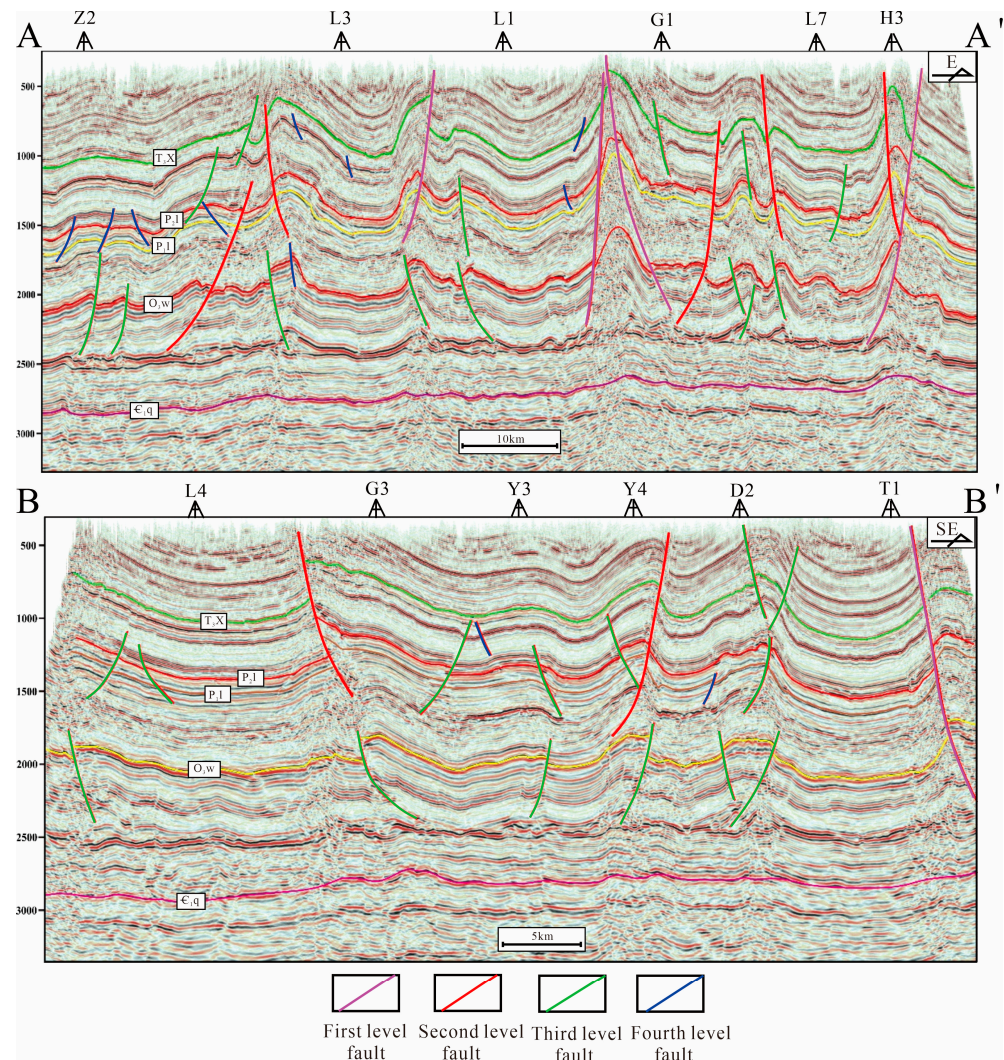


Figure 6. A structural interpretation of the seismic profile in the Luzhou area.

The faults in the Luzhou area are obviously developed. According to the fault classification standard (Table 2), the faults in the area are classified. Second and third level faults have developed in the Luzhou area. The development of first level faults in the Luzhou area are relatively small, and second level faults are only developed in the high part of the anticline, which have a significantly destructive effect on shale gas reservoirs. The syncline slope mainly develops a small-scale third and fourth level interlayer faults, which have no significant destructive effect on shale gas reservoirs. The first level faults in the area are mainly NE–SW faults, which are distributed into anticlines, such as the Tanziba, Huanggua Shan, Gufo Shan, and Dongshan tectonic units. The second level faults are mainly NE–SW, nearly S–N, and NEE–SWW, which are distributed in the transition area of the high-steep anticline and wide-gentle synclines, such as the Fuji syncline, Desheng–Baosheng syncline, and Laisu–Yunjin syncline. The third and fourth level faults are widely distributed in the structural units of the area.

Table 2. Fault classification in the Luzhou area.

Fault Level	Principle of Classification	Evaluation
First fault	A large fault that breaks upward to the surface that controls the structure.	It causes great damage to shale gas preservation. Attention should be paid to such faults in the seismic deployment, and the influence area of such faults should be deduced when calculating the favorable area.
Second fault	There are many broken layers (upwardly broken Permian or Triassic), and the drop between the upper and lower plates of the fault is large.	It has some impact on shale gas preservation conditions, but it has a great impact on drilling and other construction projects, which not only causes complex well leakage, but also makes it difficult to enter the target, or the trajectory deviates from the target layer and becomes difficult to recover.
Third fault	The internal strata of the Silurian are broken up upward, and the drop between the upper and lower plates of the fault is generally 40–100 m.	It has little effect on shale gas preservation, but to a certain extent, it will lead to trajectory out of the box, resulting in invalid footage, and should thus be avoided as far as possible in the deployment of horizontal wells.
Fourth fault	Only the Longmaxi formation is broken, and the difference between the upper and lower plates of the fault is 20–40 m.	It has no effect on shale gas preservation, but it will lead to trajectory out of the box or invalid footage. The horizontal well deployment should be avoided as far as possible, and the fault influence can also be reduced by the well drilling design and geological guidance so as to obtain a high yield.

4.2.2. Characteristics of Crack Development

We divided the natural cracks of shale in the Luzhou area into structural cracks, diagenetic cracks, and abnormal high-pressure cracks using the fine description of core cracks in the coring wells of the study area combined with imaging logging, thin-section, and scanning electron microscope data [32]. A structural crack refers to the cracking of rock caused by structural stress in the tectonic activity that is caused by crustal movement. According to the mechanical properties of the fracture and its relationship with the rock mechanics layer, structural cracks are dominated by transformational shear cracks, intraformational open cracks, and bed-parallel shear cracks. Diagenetic cracks occur along the cleavage plane under various diagenetic processes (such as mechanical compaction, dehydration shrinkage, dissolution, organic matter evolution, and rock crack), including lamellation cracks and shrinkage cracks. Abnormal high-pressure cracks are caused by abnormal high-pressure fluid breaking through the strength of organic-rich shale under the condition of sealing [33,34].

According to the FMI imaging logging data of the Wufeng–Longmaxi Formation in the Luzhou area, four groups of structural cracks, NNW–SSE, NW–SEE, NE–SW, and near S–N can be identified by the Fuji syncline (Figure 7a). NW–SE, NE–SW, near S–N, and near E–W cracks are mainly developed in the Desheng–Baocang syncline (Figure 7b). The strikes of the Laisu–Yunjin syncline cracks are mainly NW–SEE, NNE–SSW, and NEE–SEE (Figure 7c). The Fuji and Desheng–Baocang synclines are mainly oblique cracks; the middle-low angle cracks in the Laisu–Yunjin syncline play a leading role.

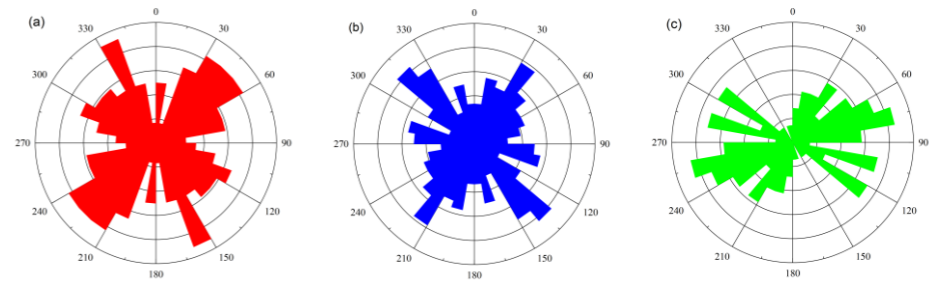


Figure 7. A rose diagram of the fracture strike of different tectonic units in the Luzhou area. (a) Fuji syncline; (b) Desheng–Baocang syncline; (c) Laisu–Yunjian syncline.

Transformational Shear Crack

Transformational shear cracks usually develop in shale that is rich in brittle minerals. The crack occurrence is usually nearly perpendicular or oblique to the shale laminae level. The crack surface is flat and straight. Multi-stage cracks intersect with each other. It is common to observe these phenomena in the core using thin-section and scanning electron microscope methods (Figure 8a,b), and these phenomena have an important influence on shale gas loss.

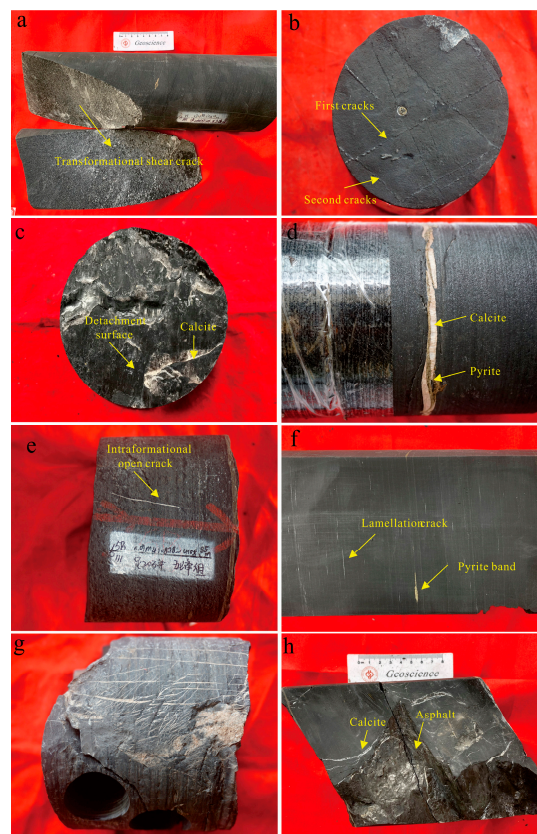


Figure 8. The characteristics of the natural crack development in the Luzhou area. (a) L2: 3724.18 m, transformational shear crack; (b) L5: 3461.67 m, the intersection of two-stage cracks; (c) L5: 3395.87 m, bed-parallel shear crack. There is a mirror slide on the crack surface and there are obvious scratches; (d) Y2: 4146.83 m, bed-parallel shear crack. Note the fibrous calcite and pyrite filling; (e) Z1: 4108.85 m, intraformational open crack. Cracks are confined between two pyrite layers; (f) L3: 4036.53 m, lamellation crack, silicon and calcite filling; (g) L4: 4053.18 m, shrinkage crack, calcite fillings; (h) L2: 3755.6 m, abnormal high-pressure crack. The crack shape is irregular, there is a high-angle development, crack face asphalt, and calcite filling.

Bed-Parallel Shear Crack

A stratigraphic shear crack, also known as a low-angle slip crack, is a kind of common structural crack developed in the weak rock mechanics of shale strata. Its occurrence is roughly parallel to the strata level, which destroys the preservation of shale gas. The bed-parallel shear cracks of the region are the most developed at the bottom of the Wufeng and Longmaxi Formations, which are usually developed on pyrite grain and surfaces with lithologic differences. Field and core identification marks are mainly marked by obvious scratches, steps, and smooth specular features on the crack surface (Figure 8c). This low-angle slip crack is mainly caused by the relative sliding between shale layers under the structural stress background of extrusion or tension. In addition, a bedding vein fracture is developed in the organic-rich shale section, which is usually filled with pyrite and fibrous calcite (Figure 8d). It is a fracture formed by fluid filling after a cleavage opens under abnormal high-pressure, and it is an important indicator of hydrocarbon expulsion in the shale.

Intraformational Open Crack

There are two mechanical formation mechanisms of an intraformational open crack, namely tension cracks and extension cracks. Tension cracks are usually characterized by an uneven bending of the crack surface, small extension scale, large span of dip angle, and length value, and a far lower overall development compared with the extension cracks. The extension cracks are generally perpendicular to the bedding plane, and the crack surface is relatively flat and regular. The cracks are limited by the top and bottom layers of the shale and generally expand along the direction of the minimum principal stress, stopping their expansion at the lithologic interface. The core usually ends in the lithology or pyrite layer (Figure 8e) and rarely crosses an interface with large differences in rock mechanical properties, which plays an important role in improving the occurrence space of free gas in shale reservoirs.

Lamellation Crack

A lamellation crack mainly refers to the crack that develops between layers or laminae and ruptures along the delamination line. Its occurrence is parallel to the interface of the lamina (Figure 8f). Lamellation cracks are usually developed in thin shale layers with dense striations, which break along the interface because of the weak mechanical properties in shale. There is a large density of these bedding cracks, which is the most common crack type in shale reservoirs. In addition, the lamellation crack opening is usually small, and the slit surface is approximately parallel to the plane with partial bending. Under the core, thin-section, and scanning electron microscope, it is often observed that the shale's bedding plane is mostly zig-zagging, extending along the edge of the particles and unable to cut through mineral particles. The interior is usually filled with calcite, organic matter, and part of the surrounding rock debris, and is connected with high-angle tensile cracks in shale, forming a more complex crack network.

Shrinkage Crack

A shrinkage crack is formed by a series of physical and chemical processes such as dehydration, shrinkage, phase transformation, or recrystallization in the process of shale diagenesis, which can be formed through purely cold shrinkage or by structural stress. It is characterized by a long extension distance and a large opening change. It often presents a wedge-shaped fracture with a steep dip angle. The cross-section is a polygon (Figure 8g), which is often filled by later sediments. It is generally developed in argillaceous sediments. Shrinkage cracks have little significance on oil and gas.

Abnormal High-Pressure Crack

An abnormal high pressure is generated in the thermal evolution process of shale organic matter and leads to the rupture of shale, thus forming shale abnormal high-pressure-

related cracks. The formation of such cracks is controlled by the content of the organic matter and the degree of thermal evolution. A high content of organic matter and high maturity parts usually develop a high degree of abnormal high-pressure cracks, such as more abnormal high pressure cracks at the bottom of the Wufeng Formation, whose occurrence, extension, and morphology greatly change and are usually filled with asphalt and calcite (Figure 8h).

4.2.3. Main Controlling Factors of Crack Development Thickness of Shale Mechanical Layer

A shale mechanical layer refers to a rock layer with similar mechanical properties. The shale mechanical layer controls the distribution of tensile cracks within the layer. The thicker the mechanical layer is, the smaller the density of tensile cracks in the layer. Core statistics show that within a certain range of rock thickness, the greater the rock thickness, the greater the crack spacing, and the smaller the rock thickness, the smaller the crack spacing. There is a negative correlation between the thickness of the shale and the density of intra-layer tensile cracks, which reflects that the mechanical thickness of shale has a significant control on the development of cracks (Figure 9a).

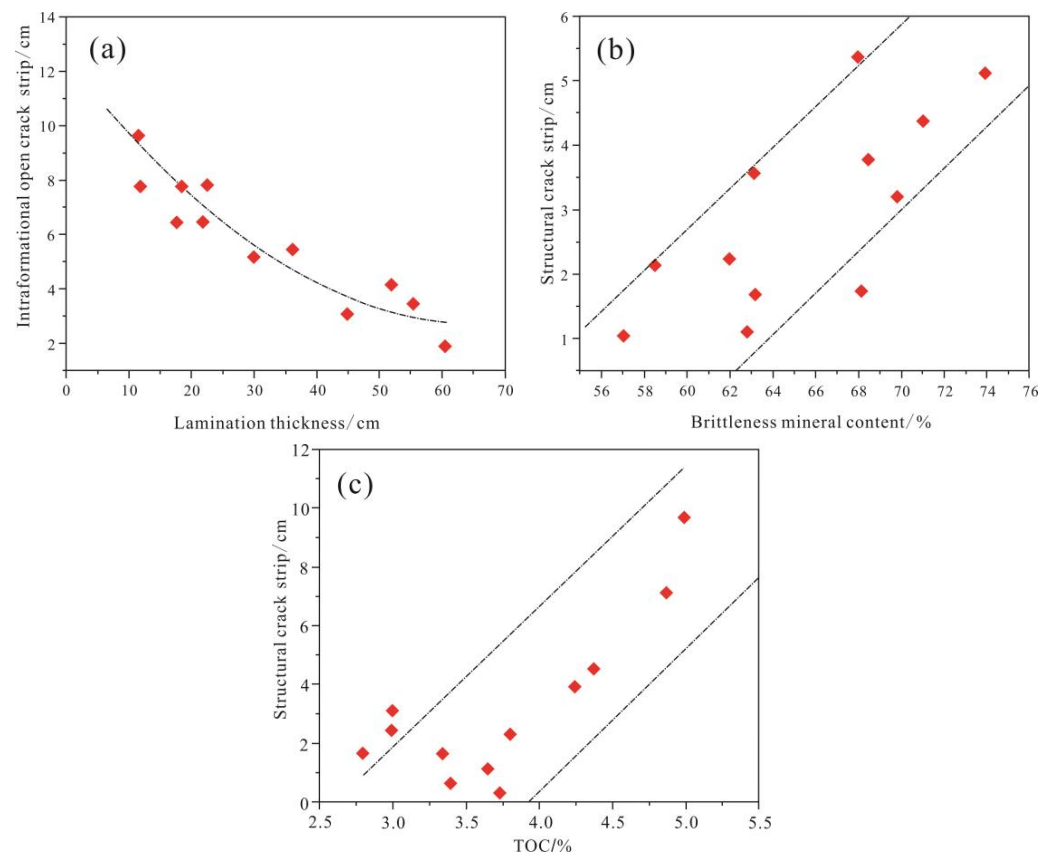


Figure 9. Crossplot of the crack line density and control factors in the Luzhou area. (a) Relationship between the tensile crack density and shale thickness; (b) relationship between the crack density and brittle mineral content; (c) relationship between the crack density and organic content.

Brittleness Mineral Content

Shale has heterogeneity, and brittleness reflects the comprehensive mechanical properties of the rock itself. At the same time, it reflects a series of petrological parameters such as the mineral composition, mineral content, cementation mode, and cementation degree of the rock. The controlling effect of the rock brittleness index on crack development is mainly reflected in that the greater the brittleness index of the rock, the more prone it is to crack

deformation, and the more prone it is to crack under the same geological conditions. There is a good linear relationship between the mineral content of the Wufeng Formation-Long 1₁ submember and the statistical crack density of the single-well structure in the Luzhou area (Figure 9b). The higher the content of brittle minerals, the greater the development of natural cracks in the shale.

Organic Content

On the one hand, the content of the organic matter in shale reservoir determines the gas content of the shale; on the other hand, it controls the development of fractures in the shale reservoir. Organic-rich shale is rich in a large number of biogenic organic silicon, which increases the brittleness of rocks. This kind of shale reservoir is prone to brittle cracks forming structural cracks under the action of structural stress, and also improves the development degree of microcracks. The study area is located in the center of the deep-water shelf. The Wufeng Formation-Long 1₁ sub-member is rich in a large number of biogenic silicon, whose silicon content is 60–70% and TOC is 2.8–6.0%. Organic-rich shale usually has a high quartz content and strong brittleness. Within a certain range, the higher the TOC content, the higher the degree of structural crack development (Figure 9c). On the other hand, the content of organic matter will affect the strength of hydrocarbon generation pressurization, resulting in the decrease of rock fracture pressure. Under the same structure stress, structural cracks and microcracks are more developed, forming a complex crack network. In addition, shale with a high TOC content is more likely to exceed the fracture pressure of the rock during the burial process, forming abnormal high-pressure cracks and dispersing a large number of acidic fluids produced by the organic matter in the process of hydrocarbon generation, leading to the formation of a large number of corrosion cracks.

4.3. Control Factors of Shale Gas Differential Enrichment

4.3.1. Effect of Uplift Erosion on Shale Gas Enrichment

Structural movement plays an important role in controlling the enrichment and destruction of shale gas. On the one hand, structural uplift leads to shale withdrawal from the hydrocarbon generation threshold and reduces shale effectiveness, resulting in insufficient gas supply in the later stage. On the other hand, the structural uplift leads to the erosion of shale overlying strata, which leads to the decrease in confining pressure and temperature of strata in Wufeng-Longmaxi Formation. With the stress change in the uplift process, the microcracks in the shale series are opened on a large scale, and the porosity and permeability are greatly improved, resulting in the enhancement of the short-range migration and accumulation of shale gas; thus, the preservation conditions of shale gas reservoirs are destroyed [35]. Generally speaking, the stronger the structural movement, the greater the uplift of the formation, the more intense the erosion of the formation, and the stronger the shale gas dissipation. In addition, the earlier the tectonic movement occurs, the greater its negative impact on shale gas enrichment is [36,37].

The burial history and thermal history of the shale in the Wufeng Formation-Longmaxi Formation of well L1, Y1, and L6 in the typical well locations of the Fuji syncline, Desheng syncline, and Yunjin-Laisu syncline in the Luzhou area are restored (Figure 10). The target horizon in the study area has undergone three structural uplift movements of different scales from the Devonian Period to the present, including during the Middle Permian, Triassic and Late Cretaceous Periods. The target horizon of the Indosinian began to enter the hydrocarbon generation threshold. With the increase of burial depth, the organic matter of the reservoir was subjected to a long-term continuous hydrocarbon generation. A large number of shale oil was cracked and entered a large number of gas generation stage, which was the main accumulation period of Longmaxi Formation. In the late Yanshanian, the deep burial ended, and the formation was dominated by a regional uplift. The formation temperature decreased, and the hydrocarbon generation stagnated. Entering the Himalayan period, this stage mainly inherited the uplift and denudation, and hydrocarbon generation is basically stagnant. The Yunjin-Laisu syncline was first uplifted about 75 Ma ago, and

then the Desheng syncline and the Fuji syncline entered the uplift stage one after the other. The uplift time was 69 Ma and 61 Ma, respectively, indicating that the Luzhou area began to uplift from east to west. Since the late Yanshanian uplift, the formation pressure coefficient of the target horizon in the Luzhou area has gradually decreased, indicating that the degree of shale gas diffusion has intensified. Similarly, compared with the shale gas content of three typical wells in the syncline, it also shows similar characteristics. That is, the earlier the tectonic uplift occurs, the greater the denudation thickness, and the shale gas content shows a negative correlation [38–40] (Table 3).

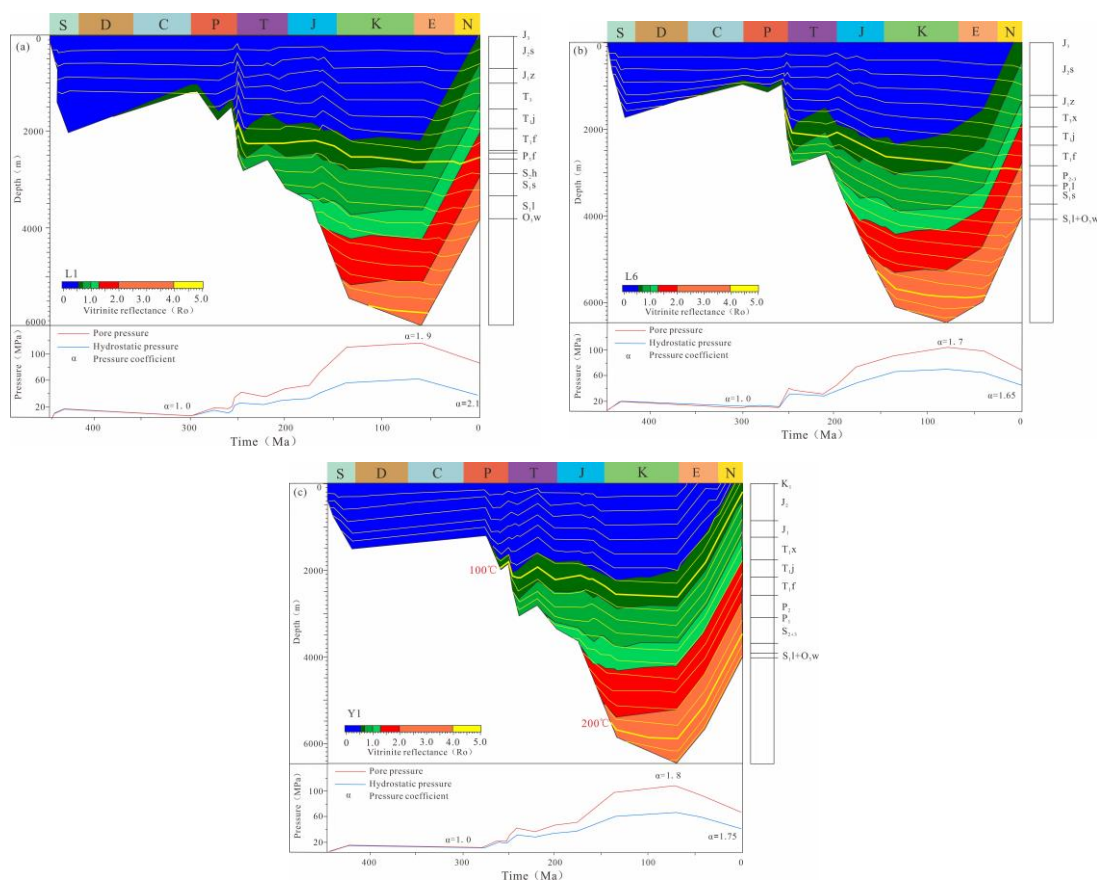


Figure 10. The burial history and thermal history of the typical wells in the Wufeng–Longmaxi Formation shale in the Luzhou area. (a) Burial history and thermal history of well L1; (b) burial history and thermal history of well L6; (c) burial history and thermal history of well Y1.

Table 3. Statistical table of the shale gas accumulation factors in different wells in the Luzhou area.

Area	Well	Uplift Rate (m/Ma)	Uplift Time (Ma)	Denudation Thickness (m)	Gas Content (m ³ /t)	Pressure Coefficient
Fuji syncline	L1	36.89	61	2250	6.70	2.10
Desheng syncline	Y1	35.80	69	2470	4.07	1.75
Laisu–Yunjin syncline	L6	33.33	75	2500	3.17	1.65

4.3.2. Influence of Tectonic Deformation on Shale Gas Enrichment

Different structural movements at different times and intensities result in different fold deformations, fracture degrees, and denudation degrees of the strata, forming different structural styles. Different structural styles result in different preservation conditions due to differences in the lateral seepage and diffusion [41]. The formation dip angle is an intuitive reflection of the tectonic strength and an important factor that affects the shale

gas enrichment. In general, shale bedding joints are relatively developed at the shale level, and the seepage effect is stronger in the bedding direction. The smaller the dip angle of the stratum is, the easier the shale gas is enriched. The experimental results show that the permeability parallel to the bedding plane is 1–40 times higher than what is perpendicular to the bedding plane in different shale formations. The bedding development of shale increases the permeability along the bedding plane, and the increase in stratigraphic dip angle will increase this phenomenon. The bedding seepage of the shale formation becomes one of the causes of shale gas loss [42–44].

The Luzhou area is a typical ejective fold belt. The main structural styles developed in the Luzhou area include fault propagation fold, thrust structure, and fault triangle structure. The structural styles of the Fuji and Desheng–Baozang synclines are characterized by the uplifting structure formed between two thrust faults. The deformation near the fault is strong, while the gentle syncline is formed on the hanging wall of the fault. The internal strain elliptic variable is small, the deformation is weak, and the preservation condition is good (Figure 11a). The characteristic structural style of the Yunjin syncline is its triangle zone structure. The lower plates of two relative thrust faults form a gentle syncline, but the interior of the syncline is greatly affected by the fault and the deformation is strong, resulting in poor preservation conditions (Figure 11b).

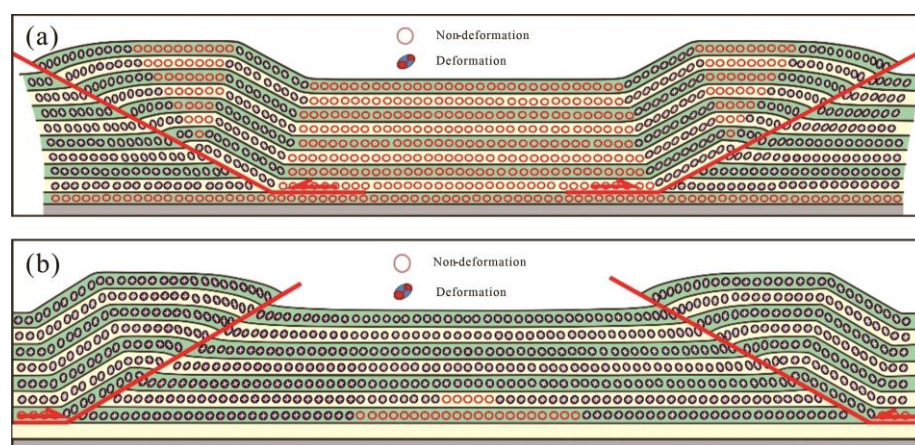


Figure 11. Internal strain distribution pattern of the structure in the Luzhou area. (a) Pop-up structure; (b) delta structure.

4.3.3. Influence of Fracture Characteristics on Shale Gas Enrichment

The influence of faults on shale gas enrichment is mainly reflected in the type, size, and connectivity of faults that can change the sealing of shale reservoirs, which leads to the differential enrichment of shale gas [45–47]. Normal faults formed in tensile environments are less close to the reverse faults formed in compressive or torsional environments. In addition, the scale of first level and second level faults are large, breaking through multiple horizons or even breaking to the surface and developing the surrounding crack system, which will lead to the loss of shale gas. The small-scale third level and fourth level faults have narrow cross-sections and are easy to fill, and they cause little damage to the shale gas reservoirs. Longitudinally, the connected fault zone composed of multiple faults will also aggravate the loss of shale gas. Cracks are a ‘double-edged sword’ for shale gas reservoirs, and they have both constructive and destructive effects. On the one hand, the formation of natural cracks can increase the occurrence space of free gas and increase the connectivity of shale pores, which can promote the reservoir capacity and production capacity of shale gas. On the other hand, the formation of cracks suggests that the region may have experienced multiple, large-scale structural movements, resulting in shale gas loss and difficulty in generating an industrial capacity [6,34].

Influence of Fault Grade on Shale Gas Enrichment

First level and second level faults in the Luzhou area are mainly formed from the Yanshanian to Himalayan Periods. First level faults break up to the surface and control the structure. There are many upward fault layers in the second level fault, and the drop between the upper and lower plates is large. For conventional oil and gas reservoirs, they can be used as a channel to transmit source rocks and reservoirs, and for shale gas this type of in situ accumulation of oil and gas resources mainly plays a destructive role. In addition, second level fault zones or serious fractures are formed near first level and second level faults, which aggravate shale gas diffusion and restrict the single-well productivity of the shale gas wells nearby [48,49].

First level faults are developed near the Tanziba structure, which cut down through the Ordovician strata and cut up to the surface, resulting in the shale of the Wufeng–Longmaxi Formation directly penetrating to the surface and resulting in a serious dissipation. The test production effect of the T1 and T2 well areas is significantly lower than that of the H2 well areas where first level and second level faults are not developed (Figure 1). The D2 well area is the most developed area, where the second level fault of the Laisu–Yunjin syncline has been revealed by drilling activities. Longitudinally, multiple faults communicate with each other, which seriously restricts the enrichment of shale gas in this well area. Its test yield is also the lowest in the Laisu–Yunjin syncline. In the Laisu–Yunjin syncline, the uplift time occurred early and the amplitude is large. In addition, the development of first level and second level faults make the adsorbed shale gas prematurely desorb and become free state gas, and the free shale gas is more likely to migrate along the high part of the page structure, which directly leads to the decrease of shale gas content and makes it difficult to form an industrial production capacity.

Influence of Distance from Fault and Fault Combination on Shale Gas Enrichment

Through the statistics of the test production of shale gas wells in the Luzhou area and the distance from different faults, we found that the higher the fault level is, the closer the distance from the fault, and the greater the influence on the preservation conditions of shale gas. The first level and the second level faults control the accumulation scale of shale gas [48]. The gas-bearing capacity of shale gas wells in the Luzhou area are poor in the range of 1200 m from the first level faults and 700 m from the second level faults. Third level and fourth level faults have little effect on the preservation of shale gas. The crack development zone near the fault is conducive to high production. The farther away from the fault, the lower the gas-bearing capacity (Figure 12). For shale gas preservation conditions, in addition to the nature and level of the faults, the fault combination has a certain impact. The combination of faults includes the combination of different properties, different periods, and different levels of faults in space. The combination of faults can reflect the structural strength and complexity of faults formed in different periods. The fault combination in a plane can be divided into parallel, small-angle, and large-angle intersections. In general, the parallel distribution of faults in an area indicates that the faults developed under similar tectonic stress conditions, while an intersecting distribution of faults indicates that the forming stages and tectonic stress conditions were different. The damage to shale gas preservation is weaker in the case of a single fault nature and simple spatial combination. The internal faults of the Fuji syncline in the Luzhou area are basically parallel, and the small-angle intersections of the combination relationship are relatively simple, and the internal structure is rich in gas. The internal faults of the Desheng–Baozang syncline intersect at large angles with a complex combination and poor gas content in the shale gas wells. The internal fault combination of the Laisu–Yunjin syncline is basically parallel, and the fault combination mode has little effect on the shale gas (Figure 12).

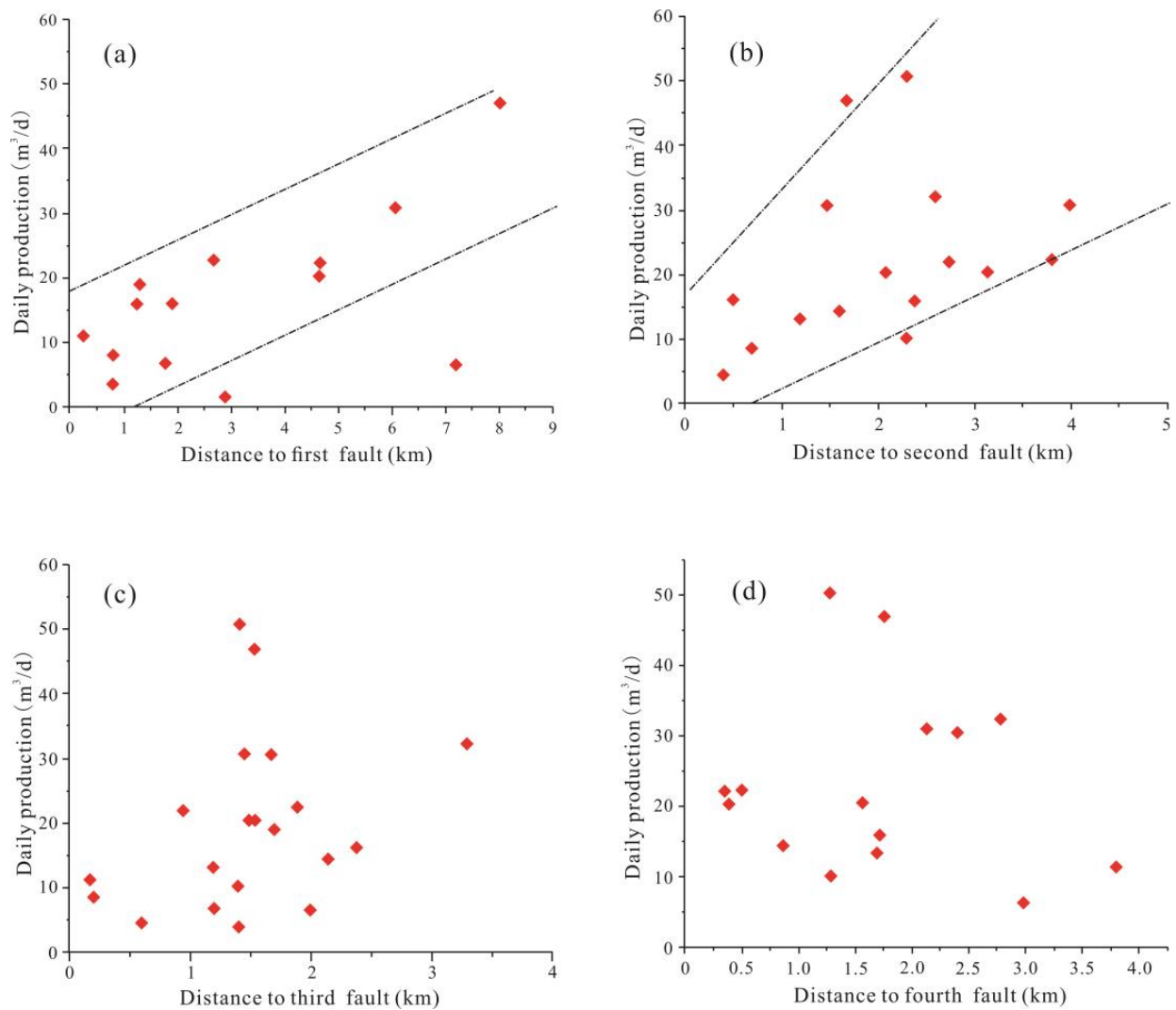


Figure 12. The relationship between the daily production and different level faults in the Luzhou area (a). Relationship between the daily production and first level faults (b); relationship between the daily production and second level faults (c); relationship between the daily production and third level faults (d).

Effect of Crack Characteristics on Shale Gas Enrichment

The single-well core fracture of the shale gas wells in the Luzhou area has been described, and the intraformational open cracks and transformational shear cracks are mainly developed in the study area. From the core of well L1 and L4 located in the Fuji syncline, the intraformational open cracks are mainly developed, the linear density reaches a 7.71 strip/m, and the gas content reaches amounts of 6.7 m³/t and 7.6 m³/t. The cracks line density of well L6 in the Laisu–Yunjin syncline are about 2.06 strip/m which is lower than that of well L1 and L4, but its gas content is 3.17 m³/t (Figure 13). The main reason for this is that high-angle cracks are mainly developed in the L6 well, which is unfavorable to shale gas enrichment. We found that the gas content of the shale gas wells decreases with the increase in the density of transformational shear cracks and increases with the increase in intraformational open cracks through the intersection diagram of the gas content, transformational shear cracks, and intraformational open cracks in the shale gas wells. Therefore, the greater the development of the transformational shear cracks, the less the shale gas content. Under the condition of having a far distance from deep

faults, intraformational open cracks play a positive role in the accumulation of shale gas (Figure 14).

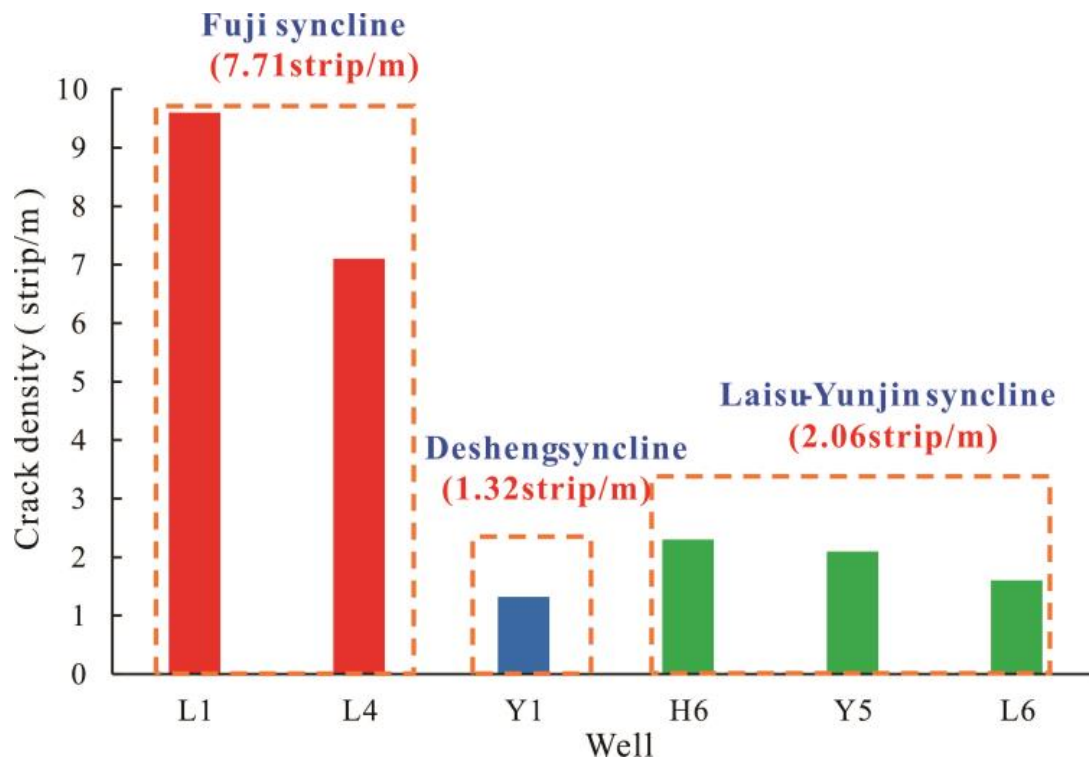


Figure 13. The fracture development degree of the different tectonic units in the Luzhou area.

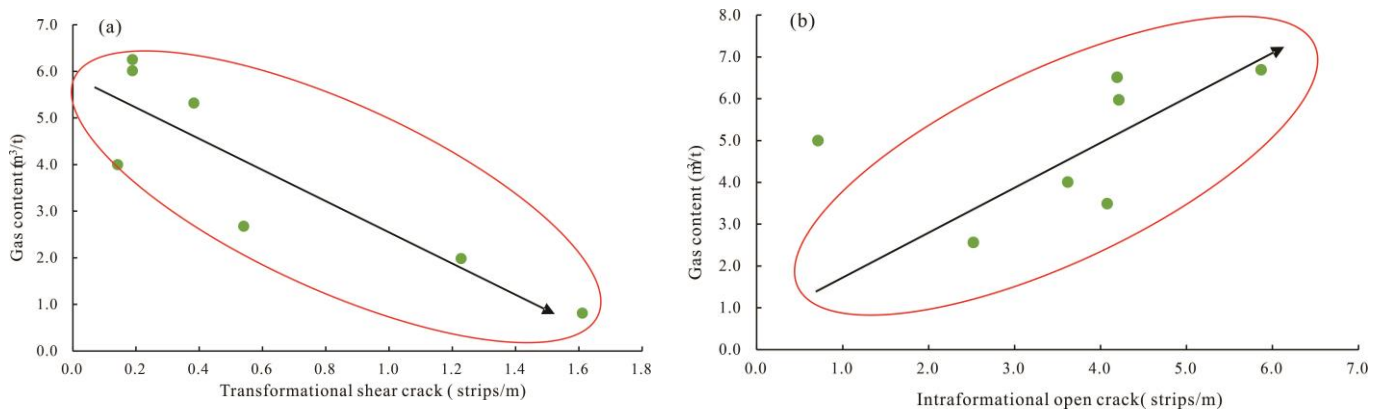


Figure 14. A crossplot of the well gas content and different cracks in the Luzhou area. (a) Intersection diagram of the gas content and transformational shear cracks. The gas content decreases with the increase of transformational shear cracks; (b) intersection diagram of the gas content and intraformational open cracks. The gas content increases with the increase of intraformational open cracks.

4.4. Differential Enrichment Model of Shale Gas

The matrix sealing of the shale reservoir in the first member of the Wufeng–Longmaxi Formation in Luzhou area is good, and the structural cracks and lamellation cracks-fractures are the dominant channel for shale gas migration. The longitudinal extension distance of the structural crack is limited, and the transverse extension distance of the lamellation crack is far. The development degree of the structural cracks, the sealing of lamellation cracks, and the migration path from the shale gas to the faults determine the enrichment or dissipation of the shale gas.

According to the different structural styles, structural deformation, evolution characteristics, fault development characteristics, uplift erosion, and other shale gas enrichment factors, the authors of [50–53] defined the distance between the two wings of the structure to be as wide as more than 10 km, and as narrow as less than 10 km. According to the dip angle of the stratum, the steepness is greater than 15°, and the slowness is less than 15°. According to the existing division, the standard formation pressure coefficient is less than 0.9 for the low-pressure gas reservoir, between 0.9–1.3 for the normal-pressure gas reservoir, between 1.3–1.8 for the high-pressure gas reservoir, and more than 1.8 for the ultra-high-pressure gas reservoir, and we combined the values with different well areas to establish the typical tectonic unit in the Luzhou shale gas enrichment model as follows [48].

1. Syncline type

The Fuji syncline as a whole is a wide-gentle syncline, with a shale reservoir buried between a 3500 and 4000 m depth; the uplift time is 61 MPa and the denudation thickness is 2320 m. There are few faults in the region. The fault strike is nearly N–S, and most of them are third or fourth level thrust faults. The fault superposition relationship is simple, and the cracks are mainly lamellation cracks. The internal damage of the syncline is small. The farther away from the first and second faults, the farther away from the erosion area and the structural parts with short dissipation durations have a higher pressure coefficient [54]. The shale gas wells have good gas content and a high production. According to the fact that the structural width of the two wings of the syncline being greater than 10 km, the average stratigraphic dip angle being less than 15°, and according to the enrichment factor, we established the enrichment model of the Fuji syncline. That is, we established the overpressure-controlled reservoir type in the core of the wide-slow syncline (Figure 15a).

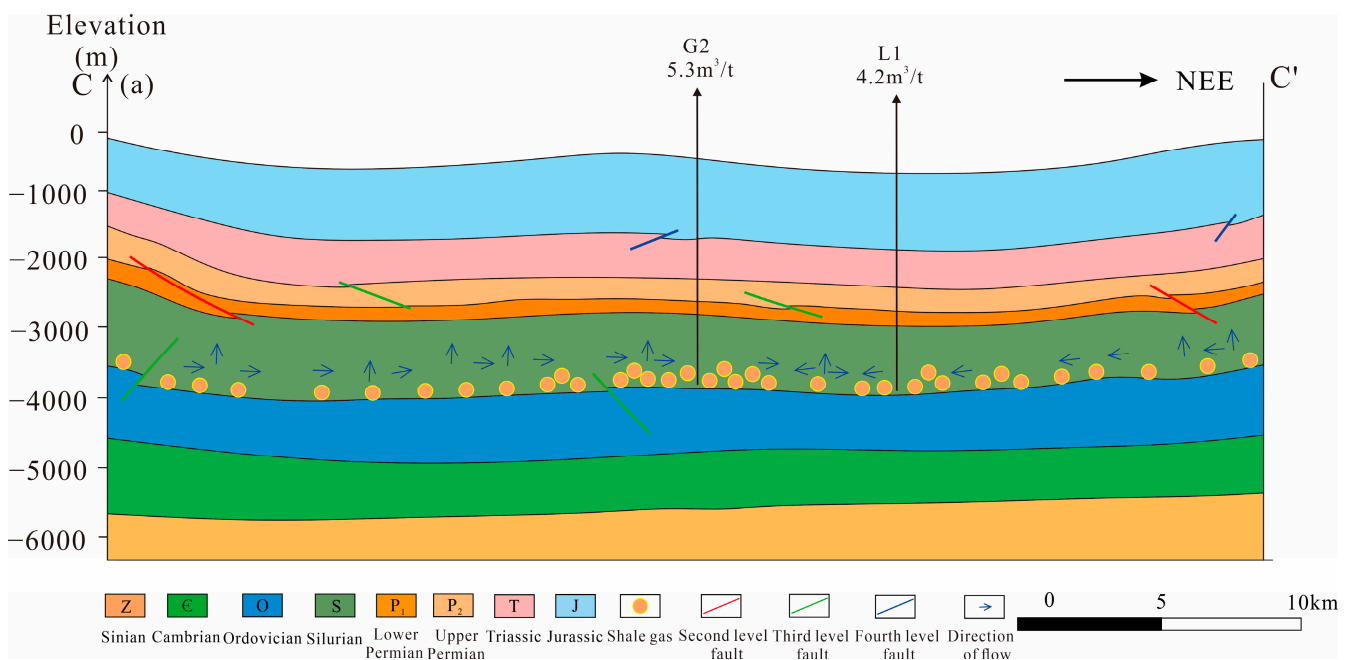


Figure 15. Cont.

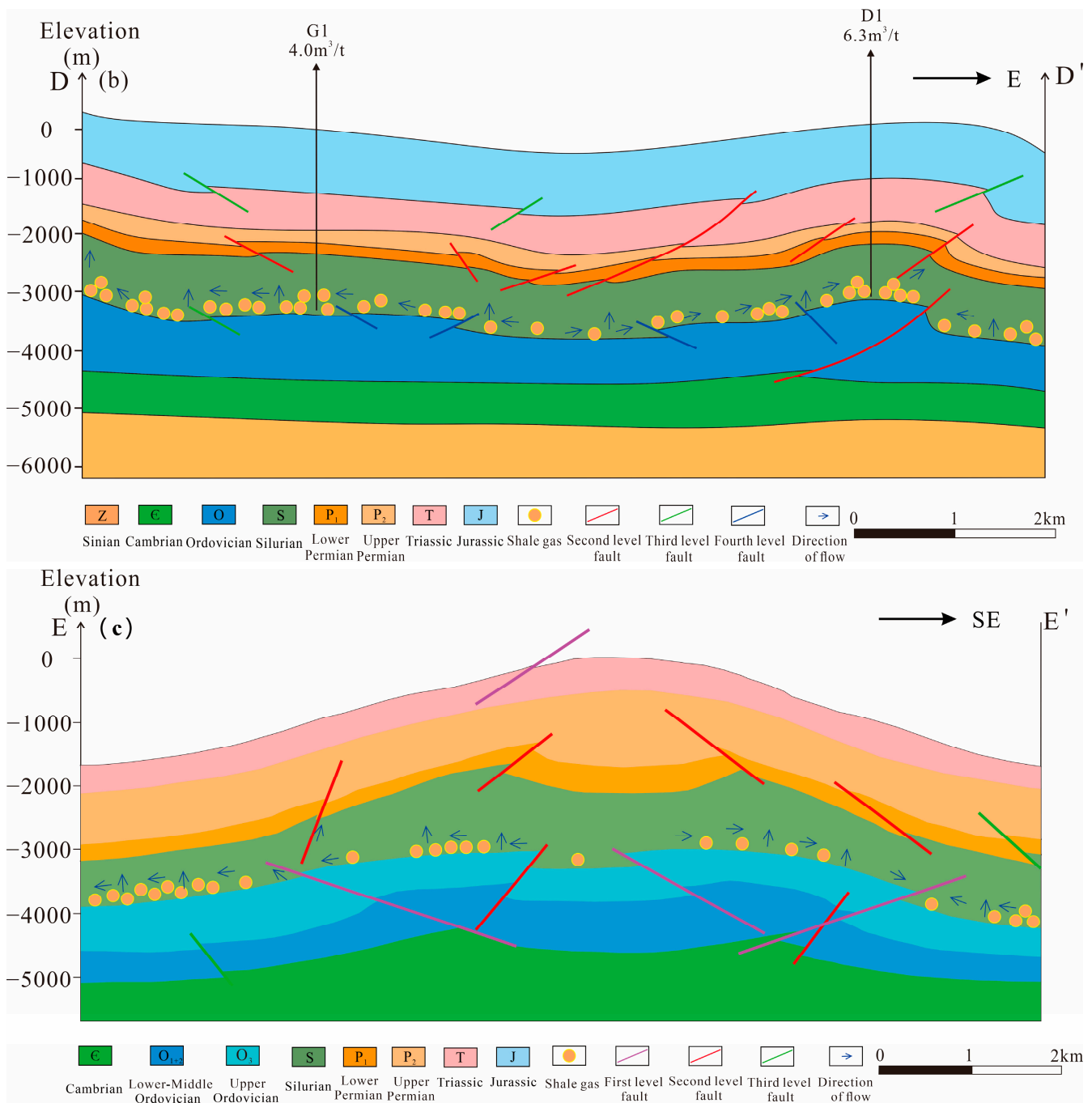


Figure 15. The shale gas enrichment model. The section position is shown in Figure 1C-C', D-D', and E-E'. (a) Fuji syncline enrichment model; (b) Desheng syncline enrichment model; (c) Gufo Shan anticline enrichment model.

The shale gas section of the Desheng syncline has a good sealing effect, good roof and floor conditions, and complete regional caprock. The uplift time is 69 MPa, denudation thickness is 2470 m, and shale reservoir depth is between 3000 and 4000 m. Most faults are low-level and have small fault spacing. The fault strike is nearly N-S direction and does not cut through the target layer, which has little effect on shale gas preservation. The crack density is relatively small, with a more than 3000 m buried depth effectively compacting the target layer, limiting the diffusion of shale gas, high formation pressure coefficient, good gas content, and shale gas enrichment. According to the structural width of the two wings

of the syncline being less than 10 km, the average stratigraphic dip angle being greater than 15° , and according to the enrichment factors, we established the enrichment model of the narrow steep syncline overpressure control reservoir (Figure 15b).

2. Anticline type

The Gufo Shan anticline is subjected to a strong tectonic compression, forming a wide and steep structural style, and there are fracture and crack developments inside the anticline. The enrichment of shale gas in the Gufo Shan anticline is mainly controlled by faults. Faults are mostly developed into second and third faults. The fault strike is nearly N–S and is close to the first and second faults. The stacking relationship is complex, which destroys the preservation conditions of shale gas. The formation pressure coefficient is medium and high, and the gas content is poor (Figure 15c).

5. Conclusions

- (1) The multi-stage tectonic movement in the Luzhou area has led to the development of NE–SW, NW–SE, E–W, and S–N superimposed structural deformations in the area. Longitudinally, the Luzhou area can be divided into the upper deformation layer, middle deformation layer, and lower deformation layer according to the structural detachment structure. On the plane, the structural form of the Luzhou area is a thin-skinned fold-thrust belt composed of a wide syncline and narrow anticline in the direction of north–south.
- (2) NE–SW-trending faults are mainly developed in the Luzhou area and nearly E–W and nearly S–N-trending faults are also developed. The faults are mainly high-angle reverse faults. According to the rock stratum level of the fault and the fault distance of the upper and lower walls, the evaluation criteria for the fault classification in the study area are established and divided into four levels. The number of first level faults in the study area is small, and the second, third, and fourth level faults are mainly developed in the area. Among them, the first and second level faults are mainly developed in the high and steep areas in the region, which have obvious destructive effects on shale gas reservoirs.
- (3) The shale of the Wufeng–Longmaxi Formation in the Luzhou area mainly develops NNW–SSE, NE–SW, and nearly S–N cracks. The Fuji syncline crack development degree is highest, where the density is 7.71 strip/m. The Laisu–Yunjin syncline crack density is 2.06 strip/m. The Desheng–Baozang syncline crack development degree is the lowest, with a crack density of 1.31 strip/m. The types of cracks are divided according to the cause of the cracks: transformational shear cracks, bed-parallel shear cracks, intraformational open cracks, lamellation cracks, shrinkage cracks, and abnormal high-pressure cracks. The thickness of the shale rock mechanical layer, brittle mineral content, and organic matter content jointly control the crack development degree of shale in the Wufeng–Longmaxi Formation.
- (4) The influence of the uplift erosion, structural deformation, fault characteristics, and crack characteristics on the shale gas enrichment of the Wufeng–Longmaxi Formation in the Luzhou area is mainly manifested in the destructive behaviors that various factors have on shale gas preservation conditions. The earlier the lifting time, the thicker the denudation thickness and the lower the gas content of the shale. The weaker the tectonic deformation intensity, the better the preservation condition, and the higher the gas content. The closer to the first and second level faults, the worse the preservation conditions, and the lower the gas content. Under the condition of having a far distance from deep faults, the bedding fractures that are developed in the target layer play a positive role in the accumulation of shale gas, and the development of cross-layer high-angle fractures will aggravate the dissipation of shale gas.
- (5) Based on the shale gas enrichment factors, two shale gas enrichment models of a syncline and anticline were established in the Luzhou area of southern Sichuan. The syncline structure is relatively stable, the roof and floor conditions are good, there is an overall development of overpressure and shale gas enrichment is affected by uplift

erosion and fracture characteristics. The structural styles of the anticlines are mostly narrow and steep anticlines with strong tectonic activity. The enrichment of shale gas is mainly affected by the fault systems.

Author Contributions: Data curation, X.S. (Xuewen Shi) and W.W.; Methodology, L.Z.; Project administration, Z.J.; Resources, M.Z.; Writing—original draft, Y.S., S.M. and X.S. (Xindi Shao); Writing—review & editing, X.T. All authors have read and agreed to the published version of the manuscript.

Funding: The National Natural Science Foundation of China (Grant No. 41802153 and 42072151) provided the funds for this study. And The APC was funded by China University of Petroleum (Beijing).

Acknowledgments: The authors would like to acknowledge the support of the National Natural Science Foundation of China (No. 41802153 and 42072151). We acknowledge the support received from the Southwest Oil & Gas Field Company. We express our appreciation for their approval to publish the data.

Conflicts of Interest: The authors declare that they have no known competing financial interests or personal relationships that could have appeared to influence the work reported in this paper.

References

- Du, W.; Yang, W.; Li, X.; Shi, F.; Lin, R.; Wang, Y.; Zhang, D.; Chen, Y.; Sun, Z.; Zhao, F. Differential Reservoir-Forming Mechanisms of the Lower Paleozoic Wufeng-Longmaxi and Niutitang Marine Gas Shales in Northern Guizhou Province, SW China: Theories and Models. *Energies* **2022**, *15*, 5137. [\[CrossRef\]](#)
- Jia, C.; Pang, X.; Song, Y. The mechanism of unconventional hydrocarbon formation: Hydrocarbon self-sealing and intermolecular forces. *Petrol. Explor. Dev.* **2021**, *48*, 507–526. [\[CrossRef\]](#)
- Jiang, Z.; Song, Y.; Tang, X.; Li, Z.; Wang, X.; Wang, G.; Xue, Z.; Li, X.; Zhang, K.; Chang, J.; et al. Controlling factors of marine shale gas differential enrichment in southern China. *Petrol. Explor. Dev.* **2020**, *47*, 617–628. [\[CrossRef\]](#)
- Song, Y.; Li, Z.; Jiang, Z.; Luo, Q.; Liu, D.; Gao, Z. Progress and development trend of unconventional oil and gas geological research. *Petrol. Explor. Dev.* **2017**, *44*, 638–648. [\[CrossRef\]](#)
- Wan, Z.; Huang, T.; Craig, B. Barriers to the development of China's shale gas industry. *J. Clean. Prod.* **2014**, *84*, 818–823. [\[CrossRef\]](#)
- Li, X.; Wang, Y.; Lin, W.; Ma, L.; Liu, D.; Zhang, Y. Tectonic Characteristics and its Effect on Shale Gas Preservation Condition in the Jingmen Region. *Front. Earth Sci.* **2022**, *9*, 1429. [\[CrossRef\]](#)
- Zou, C.; Zhao, Q.; Cong, L.; Wang, H.; Shi, Z.; Wu, J.; Pan, S. Development progress, potential and prospect of shale gas in China. *Nat. Gas Ind.* **2021**, *41*, 1–14.
- Sun, C.; Nie, H.; Dang, W.; Chen, Q.; Zhang, G.; Li, W.; Lu, Z. Shale Gas Exploration and Development in China: Current Status, Geological Challenges, and Future Directions. *Energy Fuels* **2021**, *35*, 6359–6379. [\[CrossRef\]](#)
- Dong, D.; Wang, Y.; Li, X.; Zou, C.; Guan, Q.; Zhang, C.; Huang, J.; Wang, S.; Wang, H.; Liu, H.; et al. Breakthrough and prospect of shale gas exploration and development in China. *Nat. Gas Ind.* **2016**, *36*, 19–32. [\[CrossRef\]](#)
- Shi, X.; Kang, S.; Luo, C.; Wu, W.; Zhao, S.; Zhu, D.; Zhang, H.; Yang, Y.; Xiao, Z.; Li, Y. Shale gas exploration potential and reservoir conditions of the Longmaxi Formation in the Changning area, Sichuan Basin, SW China: Evidence from mud gas isotope logging. *J. Asian Earth Sci.* **2022**, *233*, 105239. [\[CrossRef\]](#)
- Zhai, G.Y.; Wang, Y.F.; Zhou, Z.; Yu, S.F.; Chen, X.L.; Zhang, Y.X. Exploration and research progress of shale gas in China. *China Geol.* **2018**, *1*, 257–272. [\[CrossRef\]](#)
- Hu, D.; Xu, S. Opportunity, challenges and policy choices for China on the development of shale gas. *Energy Policy* **2013**, *60*, 21–26. [\[CrossRef\]](#)
- Yu, S.; Wang, X.; Li, S.; Liu, Y.; Xiao, L.; Liu, X.; Zhao, W.; Zhang, J. Impact of Geological Factors on Marine Shale Gas Enrichment and Reserve Estimation: A Case Study of Jiaoshiha Area in Fuling Gas Field. *Geofluids* **2021**, *2021*, 1–9. [\[CrossRef\]](#)
- Tonglou, G. The Fuling Shale Gas Field—A highly productive Silurian gas shale with high thermal maturity and complex evolution history, southeastern Sichuan Basin, China. *Interpretation* **2015**, *3*, SJ25–SJ34.
- Xusheng, G.; Dongfeng, H.U.; Yuping, L.I.; Zhihong, W.; Xiangfeng, W.; Zhujiang, L. Geological factors controlling shale gas enrichment and high production in Fuling shale gas field. *Pet. Explor. Dev. Online* **2017**, *44*, 513–523.
- He, D.; Li, D.; Zhang, G.; Zhao, L.; Fan, C.; Lu, R.; Wen, Z. Formation and evolution of multi-cycle superposed Sichuan Basin, China. *Sci. Geol. Sin.* **2011**, *46*, 589–606.
- Wu, J.; Liang, C.; Yang, R.; Xie, J. The significance of organic matter-mineral associations in different lithofacies in the Wufeng and longmaxi shale-gas reservoirs in the Sichuan Basin. *Mar. Petrol. Geol.* **2021**, *126*, 104866. [\[CrossRef\]](#)
- Tonglou, G.; Hanrong, Z. Formation and enrichment mode of Jiaoshiha shale gas field, Sichuan Basin. *Pet. Explor. Dev.* **2014**, *41*, 31–40.

19. Tian, H.; Zeng, L.; Ma, S.; Li, H.; Mao, Z.; Peng, Y.; Xu, X.; Feng, D. Effects of different types of fractures on shale gas preservation in Lower Cambrian shale of northern Sichuan Basin: Evidence from macro-fracture characteristics and microchemical analysis. *J. Petrol. Sci. Eng.* **2022**, *218*, 110973. [[CrossRef](#)]
20. Nie, H.; Li, P.; Dang, W.; Ding, J.; Sun, C.; Liu, M.; Wang, J.; Du, W.; Zhang, P.; Li, D.; et al. Enrichment characteristics and exploration directions of deep shale gas of Ordovician–Silurian in the Sichuan Basin and its surrounding areas, China. *Pet. Explor. Dev. Online* **2022**, *49*, 744–757. [[CrossRef](#)]
21. Zhang, G.W.; Guo, A.; Wang, Y.J.; Li, S.Z.; Dong, Y.P.; Liu, S.F.; He, D.F.; Cheng, S.Y.; Lu, R.K.; Yao, A.P. Tectonics of South China continent and its implications. *Sci. China Earth Sci.* **2013**, *56*, 1804–1828. [[CrossRef](#)]
22. Chen, S.; Zhu, Y.; Chen, S.; Han, Y.; Fu, C.; Fang, J. Hydrocarbon generation and shale gas accumulation in the Longmaxi Formation, Southern Sichuan Basin, China. *Mar. Petrol. Geol.* **2017**, *86*, 248–258.
23. Xiong, X.; Gao, R.; Guo, L.; Wang, H.; Jiang, Z. The Deep Structure Feature of the Sichuan Basin and Adjacent Orogens. *Acta Geol. Sin. Engl. Ed.* **2015**, *89*, 1153–1164.
24. Liao, J.; Zhao, N.; Chen, Y.; Tang, H.; Zheng, M.; Wu, W.; Luo, C.; Li, C.; Leng, Y. Constraints of sedimentary structures on key parameters of shale gas reservoirs: A case study of the Wufeng and Longmaxi formations of the Ordovician–Silurian transition in Luzhou area, Sichuan Basin, southwestern China. *Geol. J.* **2021**, *56*, 5691–5711. [[CrossRef](#)]
25. Zhang, Y.; Jiang, S.; He, Z.; Li, Y.; Xiao, D.; Chen, G.; Zhao, J. Coupling between Source Rock and Reservoir of Shale Gas in Wufeng–Longmaxi Formation in Sichuan Basin, South China. *Energies* **2021**, *14*, 2679. [[CrossRef](#)]
26. Xue, H.; Jiang, P.; Xu, R.; Zhao, B.; Shangwen, Z. Characterization of the reservoir in Lower Silurian and Lower Cambrian shale of south Sichuan Basin, China. *J. Nat. Gas Sci. Eng.* **2016**, *29*, 150–159. [[CrossRef](#)]
27. Li, J.; Lu, S.; Zhang, P.; Cai, J.; Li, W.; Wang, S.; Feng, W. Estimation of gas-in-place content in coal and shale reservoirs: A process analysis method and its preliminary application. *Fuel* **2020**, *259*, 116266. [[CrossRef](#)]
28. Cheng, G.; Jiang, B.; Li, M.; Li, F.; Zhu, M. Structural evolution of southern Sichuan Basin (South China) and its control effects on tectonic fracture distribution in Longmaxi shale. *J. Struct. Geol.* **2021**, *153*, 104465. [[CrossRef](#)]
29. Liu, S.; Yang, Y.; Deng, B.; Zhong, Y.; Wen, L.; Sun, W.; Li, Z.; Jansa, L.; Li, J.; Song, J.; et al. Tectonic evolution of the Sichuan Basin, Southwest China. *Earth-Sci. Rev.* **2021**, *213*, 103470. [[CrossRef](#)]
30. Feng, Q.; Qiu, N.; Borjigin, T.; Wu, H.; Zhang, J.; Shen, B.; Wang, J. Tectonic evolution revealed by thermo-kinematic and its effect on shale gas preservation. *Energy* **2022**, *240*, 122781. [[CrossRef](#)]
31. Tonglou, G.; Ping, Z. The Structural and Preservation Conditions for Shale Gas Enrichment and High Productivity in the Wufeng–Longmaxi Formation, Southeastern Sichuan Basin. *Energy Explor. Exploit.* **2015**, *33*, 259–276.
32. Zeng, L.; Lyu, W.; Li, J.; Zhu, L.; Weng, J.; Yue, F.; Zu, K. Natural fractures and their influence on shale gas enrichment in Sichuan Basin, China. *J. Nat. Gas. Sci. Eng.* **2016**, *30*, 1–9. [[CrossRef](#)]
33. Shang, X.; Long, S.; Duan, T. Fracture system in shale gas reservoir: Prospect of characterization and modeling techniques. *J. Nat. Gas Geosci.* **2021**, *6*, 157–172. [[CrossRef](#)]
34. Ding, W.; Zhu, D.; Cai, J.; Gong, M.; Chen, F. Analysis of the developmental characteristics and major regulating factors of fractures in marine–continental transitional shale-gas reservoirs: A case study of the Carboniferous–Permian strata in the southeastern Ordos Basin, central China. *Mar. Petrol. Geol.* **2013**, *45*, 121–133. [[CrossRef](#)]
35. Hu, D.; Zhang, H.; Ni, K.; Yu, G. Preservation conditions for marine shale gas at the southeastern margin of the Sichuan Basin and their controlling factors. *Nat. Gas Ind. B* **2014**, *1*, 178–184. [[CrossRef](#)]
36. Fan, C.; Li, H.; Qin, Q.; He, S.; Cheng, Z. Geological conditions and exploration potential of shale gas reservoir in Wufeng and Longmaxi Formation of southeastern Sichuan Basin, China. *J. Petrol. Sci. Eng.* **2020**, *191*, 107138. [[CrossRef](#)]
37. Yi, J.; Bao, H.; Zheng, A.; Zhang, B.; Shu, Z.; Li, J.; Wang, C. Main factors controlling marine shale gas enrichment and high-yield wells in South China: A case study of the Fuling shale gas field. *Mar. Petrol. Geol.* **2019**, *103*, 114–125. [[CrossRef](#)]
38. Liu, W.; Wu, J.; Jiang, H.; Zhou, Z.; Luo, C.; Wu, W.; Li, X.; Liu, S.; Deng, B. Cenozoic exhumation and shale-gas enrichment of the Wufeng–Longmaxi formation in the southern Sichuan basin, western China. *Mar. Petrol. Geol.* **2021**, *125*, 104865. [[CrossRef](#)]
39. Tang, X.L.; Jiang, Z.X.; Jiang, S.; Wang, H.Y.; He, Z.L.; Feng, J. Structure, burial, and gas accumulation mechanisms of lower Silurian Longmaxi Formation shale gas reservoirs in the Sichuan Basin (China) and its periphery. *AAPG Bull.* **2021**, *105*, 2425–2447. [[CrossRef](#)]
40. Nie, H.; He, Z.; Wang, R.; Zhang, G.; Chen, Q.; Li, D.; Lu, Z.; Sun, C. Temperature and origin of fluid inclusions in shale veins of Wufeng–Longmaxi Formations, Sichuan Basin, south China: Implications for shale gas preservation and enrichment. *J. Petrol. Sci. Eng.* **2020**, *193*, 107329. [[CrossRef](#)]
41. Ge, X.; Hu, W.; Ma, Y.; Li, M.; Tang, J.; Zhao, P. Quantitative evaluation of geological conditions for shale gas preservation based on vertical and lateral constraints in the Songkan area, Northern Guizhou, southern China. *Mar. Petrol. Geol.* **2021**, *124*, 104787. [[CrossRef](#)]
42. Zhang, K.; Song, Y.; Jiang, S.; Jiang, Z.; Jia, C.; Huang, Y.; Liu, X.; Wen, M.; Wang, X.; Li, X.; et al. Shale gas accumulation mechanism in a syncline setting based on multiple geological factors: An example of southern Sichuan and the Xiuwu Basin in the Yangtze Region. *Fuel* **2019**, *241*, 468–476. [[CrossRef](#)]
43. Zhang, K.; Song, Y.; Jia, C.; Jiang, Z.; Jiang, S.; Huang, Y.; Wen, M.; Liu, X.; Liu, W.; Chen, Z.; et al. Vertical sealing mechanism of shale and its roof and floor and effect on shale gas accumulation, a case study of marine shale in Sichuan basin, the Upper Yangtze area. *J. Petrol. Sci. Eng.* **2019**, *175*, 743–754. [[CrossRef](#)]

44. Zhang, K.; Jiang, Z.; Xie, X.; Gao, Z.; Liu, T.; Yin, L.; Jia, C.; Song, Y.; Shan, C.A.; Wu, Y.; et al. Lateral Percolation and Its Effect on Shale Gas Accumulation on the Basis of Complex Tectonic Background. *Geofluids* **2018**, *2018*, 1–11. [[CrossRef](#)]
45. Tang, X.; Jiang, Z.; Song, Y.; Luo, Q.; Li, Z.; Wang, G.; Wang, X. Advances on the Mechanism of Reservoir Forming and Gas Accumulation of the Longmaxi Formation Shale in Sichuan Basin, China. *Energy Fuels* **2021**, *35*, 3972–3988. [[CrossRef](#)]
46. Dai, J.; Dong, D.; Ni, Y.; Hong, F.; Zhang, S.; Zhang, Y.; Ding, L. Several essential geological and geochemical issues regarding shale gas research in China. *J. Nat. Gas Geosci.* **2020**, *5*, 169–184. [[CrossRef](#)]
47. Guo, T. Key geological issues and main controls on accumulation and enrichment of Chinese shale gas. *Petrol. Explor. Dev.* **2016**, *43*, 349–359. [[CrossRef](#)]
48. Shi, Y.; Tang, X.; Wu, W.; Jiang, Z.; Xiang, S.; Wang, M.; Zhou, Y.; Xiao, Y. Control of Complex Structural Deformation and Fractures on Shale Gas Enrichment in Southern Sichuan Basin, China. *Energy Fuel* **2022**, *36*, 6229–6242. [[CrossRef](#)]
49. Fan, C.; Zhong, C.; Zhang, Y.; Qin, Q.; He, S. Geological Factors Controlling the Accumulation and High Yield of Marine-Facies Shale Gas: Case Study of the Wufeng-Longmaxi Formation in the Dingshan Area of Southeast Sichuan, China. *Acta Geol. Sin.-Engl.* **2019**, *93*, 536–560. [[CrossRef](#)]
50. He, S.; Qin, Q.; Li, H.; Wang, S. Deformation Differences in Complex Structural Areas in the Southern Sichuan Basin and Its Influence on Shale Gas Preservation: A Case Study of Changning and Luzhou Areas. *Front. Earth Sci.* **2022**, *9*, 1383. [[CrossRef](#)]
51. Li, S.; Li, Y.; He, Z.; Chen, K.; Zhou, Y.; Yan, D. Differential deformation on two sides of Qiyueshan Fault along the eastern margin of Sichuan Basin, China, and its influence on shale gas preservation. *Mar. Petrol. Geol.* **2020**, *121*, 104602. [[CrossRef](#)]
52. He, Z.; Nie, H.; Li, S.; Luo, J.; Wang, H.; Zhang, G. Differential enrichment of shale gas in upper Ordovician and lower Silurian controlled by the plate tectonics of the Middle-Upper Yangtze, south China. *Mar. Petrol. Geol.* **2020**, *118*, 104357. [[CrossRef](#)]
53. Ma, Y.; Cai, X.; Zhao, P. China's shale gas exploration and development: Understanding and practice. *Petrol. Explor. Dev.* **2018**, *45*, 589–603. [[CrossRef](#)]
54. Guo, X.; Hu, D.; Huang, R.; Wei, Z.; Duan, J.; Wei, X.; Fan, X.; Miao, Z. Deep and ultra-deep natural gas exploration in the Sichuan Basin: Progress and prospect. *Nat. Gas Ind. B* **2020**, *7*, 419–432. [[CrossRef](#)]